General Disclaimer

One or more of the Following Statements may affect this Document

- This document has been reproduced from the best copy furnished by the organizational source. It is being released in the interest of making available as much information as possible.

- This document may contain data, which exceeds the sheet parameters. It was furnished in this condition by the organizational source and is the best copy available.

- This document may contain tone-on-tone or color graphs, charts and/or pictures, which have been reproduced in black and white.

- This document is paginated as submitted by the original source.

- Portions of this document are not fully legible due to the historical nature of some of the material. However, it is the best reproduction available from the original submission.

NASA Contractor Report 145372

SEGREGATION OF ACID PLUME PIXELS FROM BACKGROUND WATER PIXELS, SIGNATURES OF BACKGROUND WATER AND DISPERSED ACID PLUMES, AND IMPLICATIONS FOR CALCULATION OF IRON CONCENTRATION IN DENSE PLUMES

Gilbert S. Bahn

VOUGHT CORPORATION
Hampton, VA

NASA Contract NAS1-13500

May 1978

National Aeronautics and Space Administration

Langley Research Center
Hampton, Virginia 23665

SUMMARY

Two files of data, obtained with the Bendix Modular Multiband Scanner, for an acid waste dump into ocean water, were analyzed intensively. Signatures were derived for background water at different levels of effective sunlight intensity, and for different iron concentrations in the dispersed plume from the dump. The effect of increased sunlight intensity on the calculated iron concentration, calculated according to the ratio of Band 2 radiance to Band 4 radiance, was found to be relatively important at low iron concentrations and relatively unimportant at high values of iron concentration in dispersed plumes. It was concluded that the basic equation for iron concentration is not applicable to dense plumes, particularly because lower values are indicated at the very core of the plume, than in the surrounding sheath, whereas radiances increase consistently from background water to dispersed plume to inner sheath to innermost core. It was likewise concluded that in the dense plume the iron concentration would probably best be measured by the higher wave length radiances, altho the suitable relationship remains unknown.

For dispersed plumes, a technique was devised to separate background water from plume pixels, and to adjust the plume pixel radiances for distortions caused either by effective increase in sunlight intensity or by an inexplicable edge effect along the right-hand side of the scene. It was found that dense plumes yield radiances in excess of the maximum distortions in the background data, so there is no difficulty in segregating the dense plume pixels when evaluating the average radiance levels of the background water.

The techniques evolved in the course of this analysis should be generally applicable to similar sets of data.

INTRODUCTION

Quantification calculations with Bendix Modular Multiband Scanner data, obtained over an acid waste dump plume off the coast of Delaware on 28 August 1975, revealed a variety of conflicting influences in the data. Initially, efforts were made to segregate plume pixels from non-plume pixels in an empirical manner. However, as more effort was applied, it became possible to identify separately the various influences in the recorded radiances, and to deal with these in the course of quantification calculations. The following factors were found to affect the recorded radiances:

(1) the amount of total sunlight sensed by the scanner;
(2) a prominent edge effect along the right-hand edge of the scene;
(3) noise in the data, of greater magnitude in some channels than in others;
(4) the concentration of iron in the water, including one sort of characteristic for dispersed (old) plumes and a different sort for dense (fresh) plumes.

This report is a record of the work done to investigate these competing effects.

BACKGROUND WATER

Two files of data were worked with. One, referred to here as File A, represents a scene in which both old and new plumes are present, as the barge dumping the acid waste sludge is being towed on a path to intersect the dispersed plume from sludge dumped earlier. The other, referred to here as File B, represents a section of plume of intermediate age and apparently intermediate iron concentration along its core. File A was prepared as a file of every other line and every other column of original data, and consists of 400 columns and 480 lines. File B was selected as a file of 560 columns, running from tape column 241 to tape column 800, and 480 lines, covering every pixel within this field. The 560 columns of this file will be referred to hereafter as extending from column 1 to column 560, and graphed accordingly, and <u>not</u> from column 241 to column 800.

Each of these files was processed, one line at a time, to accumulate the column averages of radiances of the background water. Figures 1 and 2 show the numbers of pixels contributing to determining these column averages across the two scenes. The minimum number, of 142 at column 230 in File B, is sufficient presumably to suppress the effects of noise. In addition, for graphical representation of results, output data were averaged seven pixels at a time for File A (yielding 57 data points) and ten pixels at a time for File B (yielding 56 data points), and this too tends to suppress evidence of noise.

Early in the work with data from this mission, it had become apparent that data for Channels 1 and 10 were not acceptably reliable, and so these data were excluded from the effort reported here. Column-averaged radiances

for the background water are presented versus column number in Figures 3 and 4, for Files A and B, respectively. In both figures the uppermost line applies to Channel 3, the next line below to Channel 2, and the final six in descending order to Channels 4-9, respectively. Here and elsewhere, the radiance values are evaluated per unit of band width. All in all, considering the averaging involved, the lines appear quite lumpy. Only the marked lumps near the center of Figure 4 are readily explained, by the swift change shown by Figure 2 in the number of pixels contributing to the background average values. The most prominent features are exhibited by Figure 3, both the general increase in radiances from left to right across much of the scene, and the very marked upturns of values to the right edge. The general increase from left to right is what has been characterized as sunglitter in grey-scale photographs of the data.

Figure 3 suggests, and empirical calculations confirmed, that each of the recorded radiances can be represented as some linear function of some additive combination among them. The sum of radiances in Channels 3-8 was chosen to represent the effective level of sunlight or sunglitter. There is some evidence that Channel 2 radiances are rather noisy because of a high gain setting of the scanner for this channel, and that Channel 9 radiances are rather noisy because of truncation effect in combination with a very low gain setting of the scanner for this channel. Thus it appeared preferable to incorporate only Channels 3-8 in approximating a measure of "total" radiance of the background water, and the summation of these six values of radiance is what is referred to hereafter as Σ.

The 57 data points from File A and the 56 from File B, as represented in Figures 3 and 4, are graphed as one data set in Figures 5-12, applying to Channels 2-9, respectively. The straight lines appearing in the figures are those provided by least-squares fits to 102 of the total of 113 points, excluding the six points closest to the right-hand edge of the scene in File A (six points near the right-hand side of Figures 5-12) and excluding also the five points closest to the right-hand edge of the scene in File B (five points to left of center in Figures 5-12). The equations of these lines are:

$$r_2 = 1.7002 + 0.17621\Sigma$$

$$r_3 = 1.7070 + 0.23247\Sigma$$

$$r_4 = 0.72514 + 0.13438\Sigma$$

$$r_5 = -0.09414 + 0.17220\Sigma$$

$$r_6 = -0.63963 + 0.16737\Sigma$$

$$r_7 = -0.82591 + 0.16680\Sigma$$

$$r_8 = -0.87286 + 0.12682\Sigma$$

$$r_9 = -0.86173 + 0.10265\Sigma$$

$$r_3 + r_4 + r_5 + r_6 + r_7 + r_8 = -0.00040 + 1.00004\Sigma$$

Clearly, aside from the edge effects on the right-hand side, varying intensity of radiance of background water represents effective increase in the intensity of total sunlight. Consequently, Figure 13 has been prepared to show background water signatures for different sunlight intensities, ranging from $\Sigma = 10$ for the lowermost line, by increments of 2, to $\Sigma = 20$ for the uppermost line. This figure will be compared subsequently to a similar signature figure for dilute iron concentration.

The basic equation assigned for calculation of iron concentration was: $Fe = 2.216 - 1.049164 r_2/r_4$, with the ratio r_2/r_4 being the ratio of discrete radiances in Channels 2 and 4. Because the band widths of these two channels are not the same (0.04 for Channel 2 and 0.05 for Channel 4), the equation becomes: $Fe = 2.216 - 1.311455\ r_2/r_4$, when r_2 and r_4 are expressed per unit band width. For all of the calculations which were performed, leading to integer values of output for histogram accumulation and false-color image display, the following equation was used: $Fe = 22.66 - 13.11455 r_2/r_4$, and results then were truncated to yield integer values to the nearest tenth of a milligram per liter. The extra 0.5 unit of (10^{-1}mg/l) was carried thruout all of the calculations, and wherever results are presented as floating point numbers it must be recognized that the results are inflated to this extent.

Solutions of the equation, $Fe = 22.66 - 13.11455 r_2/r_4$, for the 113 background water data points are graphed in Figure 14 versus Σ. The data from File B are concentrated in the range of Σ from 11 to 13, whereas those from File A are spread across the figure. It is apparent from the File A results that increased sunlight intensity leads to erroneously high values of iron concentration in the background water. It is also apparent from the File B results that there is something wrong with either or both r_2 and r_4 background values for this file. Reference back to Figures 5 and 7 discloses that r_4 values are a little high, which implies that there has been some deviation from the general relationships between radiances of different channels exemplified by Figure 13. This argues for channel-by-channel, column-by-column adjustments to relate particular pollutant signals to the corresponding signals for background water.

It is both a strength and a weakness of the basic equation for iron concentration that only a ratio is involved, and no separate terms dependent upon absolute levels of radiances. One weakness is that the equation does not indicate, by its results, when it is being grossly extrapolated upward beyond its valid range, and this will be discussed subsequently. Another weakness is that the equation does not define base values of r_2 and r_4 for iron concentration, but only a base ratio (specifically, 1.72785) for zero iron. The great strength of the equation is that it was derivable from unadjusted data. It is the purpose here to show how various degrees of sunglitter affect the results at different levels of iron concentration. To do so, certain results which will be discussed later were used to fix the base level of values of r_2 and r_4. These were then increased both for sunglitter contribution and iron contribution. Results are graphed in Figure 15, versus Σ. Recalling the offset of 0.5 provided for round-off truncation, it is apparent from the bottom line that a value of Σ of 10

corresponds very closely to an iron concentration of zero (i.e., 0.5 as graphed), or, in other words, a value of 10 for Σ is approximately the base value for background water. The corresponding values of r_2 and r_4 are 4.129 and 2.442, respectively, and these yield a real value for iron concentration of -0.0014 mg/l. Therefore, the graph values corresponging to Σ of 8 are specious, and the graph should be read only from Σ of 10 upward. The assigned values of iron concentration for each line are properly the values appearing at Σ of 10. It is apparent that the effect of sunglitter diminishes as the iron concentration increases. This explains how it was that radiances unadjusted for background water served adequately in the creation of the iron concentration equation.

SEGREGATION OF PLUME PIXELS

Procedures to differentiate plume pixels from background water pixels were evolved thru many trial calculations with File A. Various parameters were employed to sort pixels into different classes, the classes were displayed with various color representations on the television screen, and determinations were made subjectively as to which classes clearly contained plume pixels, which classes clearly contained background water pixels of various kinds (normal background, sunglitter, or edge effects), and which classes were poorly defined. Parameters were varied and adjustments were made in bin limits for these parameters until a satisfactory separation was made between plume pixels and background water pixels. This was necessary not only as regards the direct designation of which were plume pixels, but also as regards the correct evaluation of background water radiances, for adjustment purposes. Eventually, a satisfactory segregation of plume pixels from background water pixels was effected, and it became possible to evaluate the column-averaged radiances for all background water. Once this was done, calculations could proceed on the basis of adjusted radiances.

An array of background radiance values such as shown in Figure 3 was inspected, and values at a particular location were selected as base values for subsequent work. This was done prior to the least-squares fitting represented in Figures 5-12, so the base values selected are not quite the same as those which would be chosen at present. The values which were selected are compared below to those provided by substituting a value of 10 for Σ into the set of least-squares equations:

Channel	Values selected earlier	Values computed presently
2	3.434	3.462
3	4.050	4.032
4	2.040	2.069
5	1.713	1.628
6	1.144	1.034
7	0.961	0.842
8	0.512	0.395
9	0.256	0.165
Σ	10.420	10.000

The computational procedure that was followed, for adjustment of the raw data, involved subtracting the column average background radiance from the individual pixel radiance, and adding this difference to the assigned base value. It should be noted that this procedure would be valid only for cases where, aside from noise, the background radiances are sensitive only to column location, and not to line location. Such were the conditions found in Files A and B.

Using the assigned base values, as recorded above, and the empirically derived segregation technique, calculations of iron concentration were made for all of the plume pixels of File A, using adjusted values for r_2 and r_4. The results were sorted into classes of increment 0.1 mg/l of iron, and the adjusted radiances were accumulated, so that the average adjusted radiance for each channel (2 thru 9) in each class was determined. Results are presented in Figures 16-23, applying to Channels 2 to 9, respectively. The class radiance is plotted versus the class value for iron concentration as calculated from the mean values of r_2 and r_4. In each figure there is a line representing a least-squares fit to a number of the data points, which number ranged from a minimum of five for Channel 2 (Figure 16) to the maximum of eight, for all eight data points, for Channels 6-9. In Figure 24 the sum of the adjusted radiances in Channels 3-8 (i.e., Σ as previously defined) is graphed versus iron concentration, and the line for the least-squares fit of these data is included, based upon the first seven points.

The equations for radiance as a function of iron concentration are:

$$r_2 = 3.7763 + 0.022824\ Fe$$
$$r_3 = 3.9895 + 0.18573\ Fe$$
$$r_4 = 2.1729 + 0.13410\ Fe$$
$$r_5 = 1.6650 + 0.15667\ Fe$$
$$r_6 = 0.93108 + 0.13128\ Fe$$
$$r_7 = 0.76585 + 0.10653\ Fe$$
$$r_8 = 0.33944 + 0.06373\ Fe$$
$$r_9 = 0.13383 + 0.039104\ Fe$$
$$\Sigma = 9.9076 + 0.75930\ Fe \text{ (vs. } 9.8638 + 0.77804\ Fe \text{ by summation)}$$

The pixels represented by these equations were all in the dispersed plume of File A. Noise aside, it appears that any one of the equations could be used to compute iron concentration from the adjusted radiance of any one channel. To minimize the effects of noise, it was considered desirable to use more than one radiance in combination to perform such a computation. Accordingly, six of the equations were inverted:

$$Fe = 5.3842r_3 - 21.480$$
$$Fe = 7.4571r_4 - 16.204$$
$$Fe = 6.3828r_5 - 10.627$$
$$Fe = 7.6173r_6 - 7.9023$$
$$Fe = 9.3870r_7 - 7.1891$$
$$Fe = 15.6912r_8 - 5.3262$$

The equations involving r_3, r_4, and r_5 were combined, and separately the equations involving r_6, r_7, and r_8 were combined, to yield two separate equations for calculation of iron concentration from adjusted radiances:

$$F1 = 1.7947r_3 + 2.4857r_4 + 2.1276r_5 - 16.104$$
$$F2 = 2.5391r_6 + 3.1290r_7 + 5.2304r_8 - 6.536$$

The solutions are plotted versus iron concentration according to the ratio of r_2 to r_4 in Figure 25, where the line added is the line of identity. It is apparent that, using adjusted data, all three solutions for iron concentration in the dispersed plume yield equivalent results. Signatures for various levels of iron concentration in the dispersed plume, according to the foregoing equations, are graphed in Figure 26.

If everything fit together perfectly, the lowermost signature on Figure 26 would coincide with the lowermost signature on Figure 13. Both signatures are supposed to apply to pure background water with no sunglitter. The signatures do compare very favorably, but not identically. Following are the comparable radiances:

Channel	Background Water for Σ of 10	Zero Iron Concentration
2	3.462	3.776
3	4.032	3.990
4	2.069	2.173
5	1.628	1.665
6	1.034	0.931
7	0.842	0.766
8	0.395	0.339
9	0.165	0.134

When Figure 15 was introduced, it was stated that results to be discussed later had been used to fix the base level of values of r_2 and r_4, to which various effects of sunglitter were added. What was done in this case was to assign values to Fe in order to compute values of r_2, r_3, r_4, and r_5, from which were calculated both Fe according to the ratio of r_2 to r_4 and F1 according to the contributions of r_3, r_4, and r_5. The output value for F1 was identically the input value assigned for Fe. The output value for Fe was not identical to the input value assigned. This is why Figure 15 was introduced with the perspective that the base values of Fe are those prevailing at Σ of 10, which are not a uniformly spaced set for the six lines of the figure. Further discussion of the relation between Fe from r_2/r_4 and F1 is reserved until the final processing of Files A and B is taken up.

The formulation of the separate parameters F1 and F2 followed upon the empirical efforts at segregation of plume pixels from background water pixels. It was determined that, for radiances which might represent dispersed plume pixels or which might represent sunglitter, the relative values of F1 and F2 will reveal which are plume pixels and which are not. Specifically, if F2 exceeds F1, and if F1 is greater than zero, but less

than twelve, the pixel is a background water pixel. (If F1 is less than zero, the pixel is automatically a background water pixel, and if F1 is greater than twelve, the pixel is automatically an acid plume pixel.) The comparison of F1 and F2 values can be made iteratively, commencing with an initial calculation in which no adjustment is made to the raw data for radiances. This initial calculation will assign most, but not all, of the background water pixels to the background category for calculating the column-averaged background water radiances. For the next calculation, these background water radiances can be employed to compute F1 and F2 from adjusted radiance values, thus affording better definition of the background water category, and thus outputting better column-averaged background water radiances for use in the next iteration. It was found, working with both File A and File B, that two or three iterations after the initial calculation were sufficient to define the background water radiances with suitable precision.

Listed following are the mean absolute differences in the background radiances of the various channels as iteration proceeded:

File A

Channel	First Results - Base Level	Second Results - First Results	Third Results - Second Results
2	0.685	0.019	0.002
3	0.819	0.028	0.003
4	0.477	0.020	0.002
5	0.533	0.021	0.002
6	0.510	0.019	0.002
7	0.494	0.017	0.001
8	0.357	0.013	0.001
9	0.289	0.009	0.001

File B

Channel	First Results - Base Level	Second Results - First Results	Third Results - Second Results
2	0.454	0.069	0.009
3	0.505	0.044	0.016
4	0.355	0.022	0.011
5	0.247	0.019	0.010
6	0.226	0.065	0.007
7	0.201	0.054	0.006
8	0.124	0.057	0.004
9	0.095	0.035	0.004

For File A, the final processing was performed using the results of the second iteration to adjust for background water variability. For File B, the final processing used the results of the third iteration. The results presented in Figures 1-12 all apply to the second iteration for both files.

Summarizing the segregation scheme:

(1) initially with no corrections, F1 and F2 values are computed from the raw data for radiances
(2) background water pixels are identified, and column-averaged values are computed
(3) a new calculation is made, adjusting the individual radiance values for variability in the background water, and again computing F1 and F2 values
(4) background water pixels are identified according to the F1 and F2 values based on adjusted radiances, and column-averaged values, unadjusted, of course, are again computed for the background water.

Steps (3) and (4) are repeated as many times as desired until there is no practical change in the characteristics of the background water. Then, final calculations are performed. In these final calculations, the segregation process may be carried out with adjusted data and the calculation of iron concentration may be carried out with unadjusted data, as desired.

In actual practice, because of what has been deemed noise considerations, when the value of F2 did not exceed the value of F1 by more than 0.1 mg/l, the pixel was assigned as a dispersed plume pixel (i.e., if F1 exceeded zero). This adjustment was determined by providing separate categories for F2 = F1, F2 = F1 + 0.5, and F2 = F1 + 1.0, and inspecting the resulting effects as to their filling in the dispersed plume and contributing noise (elevated iron concentration) to the background water.

CALCULATIONS OF IRON CONCENTRATION

The primary results to be discussed herein are those obtained by processing both files of data to calculate iron concentration for plume pixels according to the basic equation based on the ratio r_2/r_4. Consistently with the derivation of this equation, these calculations were performed with unadjusted data for r_2 and r_4, whereas the segregation scheme to identify plume pixels was operated with adjusted data, as has been described above. Where the value computed for F1 was in excess of 12, the pixel was automatically assigned as an acid plume pixel. Where the value of F1 was less than zero, the pixel was automatically assigned as a background water pixel, which amounted to 51% of the scene for File A and 45% for File B. For values of F1 ranging from zero up to 12, values of F1 and F2 were compared to determine which class set to assign the pixel to.

One class set consisted of background water. The pixels in this set exhibited some degree of effective sunglitter even after adjustment of radiances according to the column-averaged data; otherwise, F1 would have exceeded F2. For File A, the evidence of sunglitter persisted as a pattern in the right-hand portion of the scene, whereas for File B the evidence of sunglitter is perceived as irregular banding across the scene. In both cases, 34% of the pixels fell into this class set.

The principal class set for dispersed plume pixels was composed of those pixels for which F1 did exceed F2. If 100 pixels is arbitrarily taken as the cutoff point for significance, then iron concentrations in the dispersed plume ranged up to 0.7 mg/l for File A and to 1.0 mg/l for File B. For File A, 8.5% of the scene fell into this set of classes, and for File B, 11.9% of the scene was so classified.

As noted earlier, two additional sets of classes were provided for, in attempting to ensure that the proper delineation was made between dispersed plume and background water pixels. The first of these additional sets incorporates those pixels for which F2 exceeds F1 by up to 0.5, and the second incorporates those pixels for which F2 exceeds F1 by more than 0.5 but no more than 1.0. (As has been stated, when F2 exceeded F1 by more than 1.0, the pixel was assigned to the background water set, already discussed.) These two additional sets of classes were identified visually as dispersed plume classes generally located along the borders between plume and surrounding water. Together, they comprised 5.4% of the scene for File A and 4.5% of the scene for File B. The values of iron concentration which were calculated ranged up to 0.6 mg/l for File A and up to 0.7 mg/l for File B. Output values of F1 were generally comparable.

There remain for discussion those pixels for which F1 calculated in excess of 12, 1.2% of the scene for File A and 5.1% of the scene for File B. In the development of the segregation technique, it was fortunate that the work was performed on File A, because there are abrupt numerical distinctions between the dispersed and dense plumes in that scene, and it was possible to recognize that almost every pixel of very high value of Σ was a dense plume pixel. A dense plume pixel is now hereby defined as a pixel for which F1 exceeds 12 and for which also F2 exceeds F1. A pixel for which F1 exceeds 12 and F1 also exceeds F2 is designated a dispersed plume pixel of high iron concentration.

In the case of File A, 29 pixels out of 192000 have values of F1 in excess of 12, and also in excess of F2, wherefore they classify as dispersed plume pixels of high iron concentration. These are trivial in number for the present discussion, but will be referred back to later. It was not anticipated that most of the pixels in File B for which F1 exceeds 12 would classify as dispersed plume pixels (F1 exceeds F2), but such proved to be the case. However, somewhere around twenty per cent of these core pixels in File B, located in the deepest heart of the core, classified the same as the dense plume pixels of File A, that is, with F1 in excess of 12 and F2 in excess of F1. Reflecting upon these facts, it seems conceivable that if there were both excessive sunglitter (or edge effect) and dense plume in the same columns of a scene, it might not be possible to separate out the background water adequately. On the other hand, File A did seem to present an extreme case of distortion of background data (cf. Figure 3), and it is reasonable to hope that no worse a condition would arise in future missions. Since File A was indeed segregated successfully, the segregation technique is anticipated to be applicable generally, but this precautionary note about interaction of dense plume

radiances and extreme sunglitter radiances deserves to be recorded.

For both File A and File B, iron concentrations up to 1.2 mg/l were calculated for the pixels for which F1 exceeded 12. The bulk of the evidence to be presented graphically suggests that these solutions are not valid. For one thing, the equation for iron concentration is being extrapolated into a regime of values of r_2 and r_4 well beyong the regime for which the equation was derived. For another, it is known that the higher wave length radiances increase greater, proportionally, than the lower wave length radiances as the iron level moves from dilute to concentrated, contrary to the trends of Figures 16-23. Therefore, it may at least be supposed that the relationship between r_2 and r_4 prevailing at dilute iron concentrations does not continue into the regime of elevated iron concentrations. At the same time, it must be acknowledged that F1, deemed to be a valid measure of iron concentration in dispersed plumes, will not necessarily extrapolate in a valid manner itself into the regime of elevated iron concentrations. However, it does seem fair to propose that increase in value of F1 (or of F2) will continuously indicate some measure of increase in iron concentration. This will be discussed subsequently in greater detail. However, it is appropriate to begin consideration of the calculations of iron concentration for Files A and B by comparing the values of F1 with the values provided by the basic equation involving r_2/r_4. These results are presented in Figure 27, where F1 is graphed versus the iron concentration provided by the basic equation. Both ordinate and abscissa values were computed from the various class mean values of unadjusted radiances, which were derived from the processing of the two files to determine the integerized concentration of each individual plume pixel. Considering that unadjusted data have been employed, identity of results would not be expected, and the agreement of results for values of F1 up to about 12 is generally satisfactory. However, it is apparent that for higher values of F1, the results are not meaningful. In the upper outline of points for values of F1 above 16, the upper side represents solutions from File A and the lower side represents solutions from File B. Clearly, the principal difficulty is that the basic equation for iron concentration does not apply to concentrated plumes, for which values of F1 greater than 12 are calculated. Interpreting the figure in another way, pixels with calculated iron concentrations in excess of about 1.0 mg/l are surely suspect, and any pixels which are visually known to lie in areas of higher concentration than these suspect pixels are themselves even more suspect in value.

The mean unadjusted radiances from the processing of Files A and B, corresponding to the results presented in Figure 27, are graphed in Figures 28-35. It is obvious that agreement between each radiance and the iron concentration is generally as one would expect for dilute values of iron concentration, and as much without meaning as was Figure 27 for high values of iron concentration.

One further result from basic processing of Files A and B must be presented at this point. The computer program could be run to evaluate iron concentration with either unadjusted or adjusted values of r_2 and r_4, and, separately, could accumulate either unadjusted or adjusted radiances in

evaluating the class average values of radiance. Reruns were made where the iron concentration was, as before, calculated from unadjusted radiances, so as to define classes of identical composition, but where those class characteristics were now evaluated in terms of adjusted radiances. In Figure 36 there is graphed the iron concentration calculated from mean adjusted class radiances versus the value calculated from mean unadjusted class radiances. The line for least-squares fitting of the data is included. The equation of this line is

$$Fe_{\text{adjusted data}} = -0.63148 + 1.0985\ Fe_{\text{unadjusted data}},$$

and the absolute average residual amounts to 0.403. It is apparent that the distinction between employing adjusted or unadjusted data is not the source of difficulty revealed by Figures 27-35. It is also apparent that the use of adjusted data to initiate the preparation of Figures 16-26 represented relatively minor distortion of the fundamental relationship between sea truth data and unadjusted radiances which had been extracted in formulating the basic equation for iron concentration.

PROCESSING IN TERMS OF F1

The premise was pursued that increase of iron concentration should lead to increase of radiance in each channel, indefinitely, altho not necessarily linearly and perhaps not even significantly at high values of iron concentration. The underlying question in this pursuit was as follows: Is it more logical that ultimately there should be no further increase in radiance with increased iron concentration, or that ultimately there should be no further increase in iron concentration with increased radiance? The inversion of this second alternative is the question whether there is some iron concentration for which the radiance in each channel becomes infinite, and the obvious answer to this question is negative. Some results to be presented here falsely indicate a positive answer, and thus reveal further the difficulty in extrapolating the basic equation for iron concentration into the regime of high values. The results also argue for endeavoring to describe high iron concentrations in qualitative terms by means of computed values of F1 or of F2.

These calculations were made on File A. Classes were defined according to integerized values of F1, rather than Fe. The same sets of classes of dispersed plume pixels were provided for as in the previous processing, that is, one set for which F1 exceeded F2, a second set for which F2 exceeded F1 by no more than 0.5, a third set for which F2 exceeded F1 by more than 0.5 but no more than 1.0. Also there was the background water set for which F2 exceeded F1 by more than 1.0. As before, those pixels for which F1 was less than zero were automatically classified as background water.

All pixels with values of F1 in excess of 12 were dealt with separately. Recall, from Figure 27, that there were no resulting classes with integer values in excess of 12, when the basic equation was used to compute iron concentration from the ratio r_2/r_4. Now, automatically, all of these pixels were ordained to form classes with values in excess of 12, since this value of 12 was the dividing point for such a series of classes,

defined by values of F1. Actually, two such series of classes were provided for, one with F1 greater than F2 and the other with F2 greater than F1.

The numerical distinction between dispersed plume and dense plume in File A was remarked about before. For values of F1 less than 12, with 100 pixels minimum used as the cutoff, the iron concentration ranged only up to 1.0 mg/l. A scattered few pixels calculated at 1.1 mg/l, and the program identified none at 1.2 mg/l. It has also been noted before that 29 pixels in File A have values of F1 in excess of 12 and values of F1 in excess of F2. It was found that 21 of these pixels can define 9 classes with approximately valid data, whereas the other 8 pixels have radiance counts (raw data) pegged out at the maximum scale value, and thus are inadmissible. There are 2319 dense plume pixels, for which F1 exceeds 12 and F2 exceeds F1. Of these, 86 have radiance counts pegged out at the maximum scale value, and must be discarded. The other 2233 of these pixels define 17 classes with integerized values ranging from 13 to 29.

Adjusted radiances were accumulated as the calculations proceeded, and class mean values were determined, from which values of F1, F2, and Fe were computed. In Figure 37, F1 is graphed versus Fe. Circles are used for the 36 classes corresponding to values of F1 less than 12. Squares are used for the 9 classes which represent dispersed plume of high iron concentration; these points appear to exhibit no trend. Triangles are used for the 17 classes which represent dense plume. The circles and triangles, taken together, appear to define a curve which begins with gradual slope and becomes essentially vertical at an abscissa value between 10 and 11. In Figure 38, F2 is graphed versus Fe, using the same set of symbols as before. The indication by the circles and the triangles of one curve which becomes essentially vertical is even more pronounced than was the case in Figure 37. In Figure 39, F2 is graphed versus F1, with the same set of symbols. Here, the squares extend the trend of practical equality between F1 and F2 which the circles, by their class definitions, enforce. On the other hand, a separate line is defined by the triangles for the dense plume classes, showing distinction for dense plume at values of F1 greater than about ten. Now one must concede that F2 is evidently a better measure of iron concentration in the dense plume than is F1, altho this is not meant to claim that F2 is a <u>linear</u> measure at the high concentrations which it implies.

To present the individual radiance values from these calculations, F1 or F2 might have been employed as the abscissa. However, since it cannot be claimed that either of these parameters is a known measure of iron concentration in the dense plume, there is no real benefit to such a display of results. Therefore, Fe has been used as the abscissa in preparing Figures 40-47, which represent the mean adjusted radiances for Channels 2-9, respectively incorporating those classes which had been represented by circles or triangles on Figures 37-39. These present figures for radiance make much more sense than did Figures 28-35. Consistent with Figures 37-39, they indicate that Fe is a reasonable measure of iron

concentration up to values of about 10 (i.e., 1.0 mg/l), i.e., generally in the dispersed plume, whereas it is simply not applicable to the dense plume. The evidence of vertical climb of radiance, at values of Fe between 10 and 11, demonstrated by Figures 43-47 (Channels 5-9) simply requires that these values of Fe be rejected; one cannot conceive of infinite radiance at an iron concentration of about 1.1 mg/l, and the evidence of Figure 36 fairly assures that the difficulty here is not the use of adjusted rather than unadjusted radiances.

If the values of Fe above 10 are to be rejected, as just done, then no trends of significance are to be discerned from Figures 40 and 42 for the radiances which contributed to the calculation of such values. However, it is interesting that, at values of Fe between about 6 and about 10, r_2 (Figure 40) seems to decline a little, r_3 (Figure 41) seems to flatten out, and r_4 (Figure 42) seems to maintain the same slope as for lower values of Fe, all of which contrast with the upswings in values of r_5 to r_9 in this same range of Fe from 6 to 10, as exemplified by Figures 43-47. What physical explanation there may be for failure of any radiance to increase, at least to some infinitesimal degree, with increase of iron concentration, cannot be envisioned. It thus seems likely that Figures 40 and 41 reflect vagaries in the actual data of File A, instead of an explainable phenomenon.

Presumably the principal interest in quantification of digital imagery for acid waste plumes will be in determining the spread and dissipation of known plumes, and not in the hydromechanics of their formation. In this sense, the equation for Fe is adequate. In qualification, it only seems necessary to caution that calculated values of iron concentration approaching 1.0 mg/l may be somewhat distorted from the true values, and that calculated values in excess of 1.0 mg/l should be taken as outlining dense concentrations, at the cores of which may be calculated definitely false values even ranging below 1.0 mg/l.

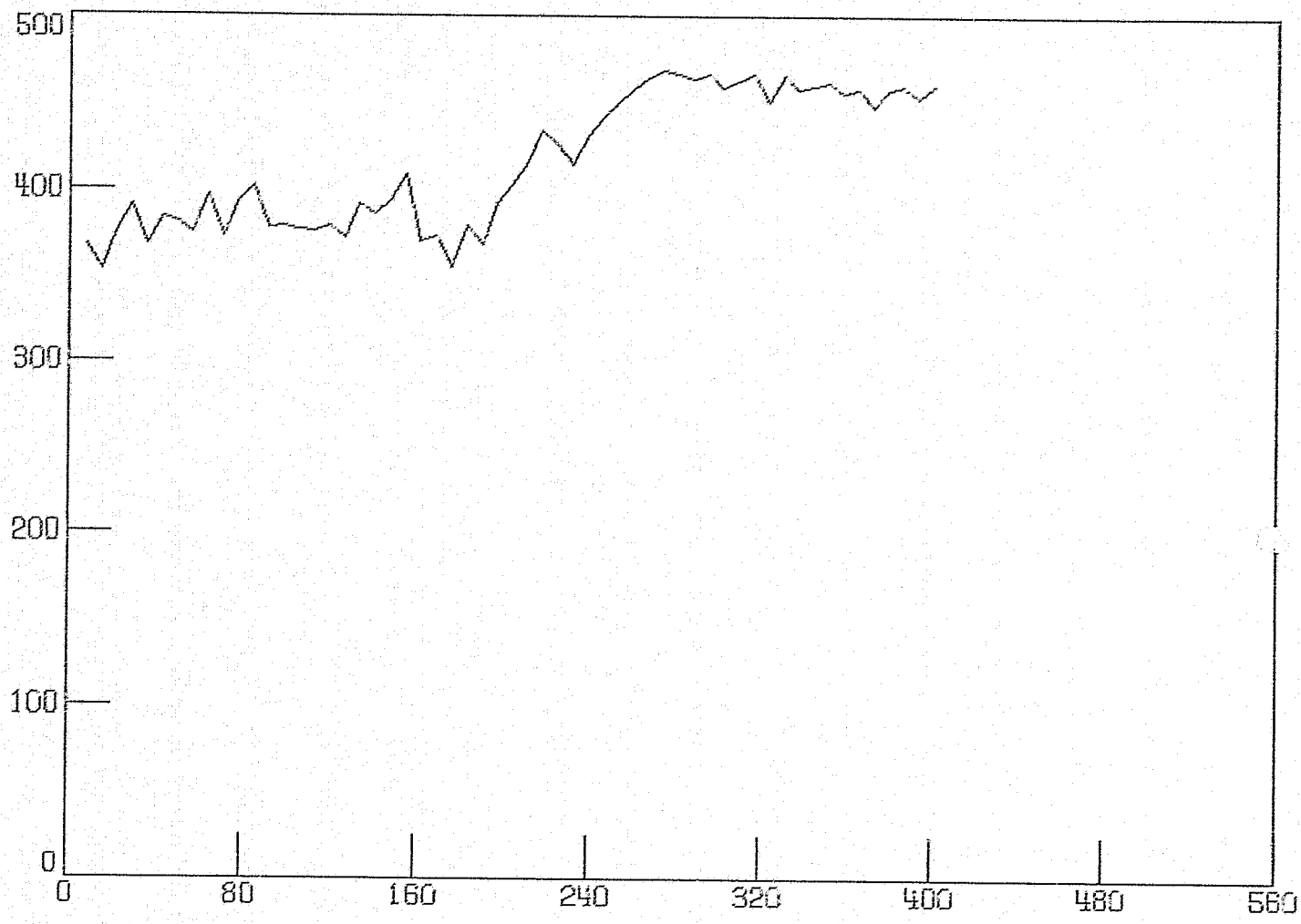

Figure 1. File A: Number of Background Water Pixels vs. Column Number.

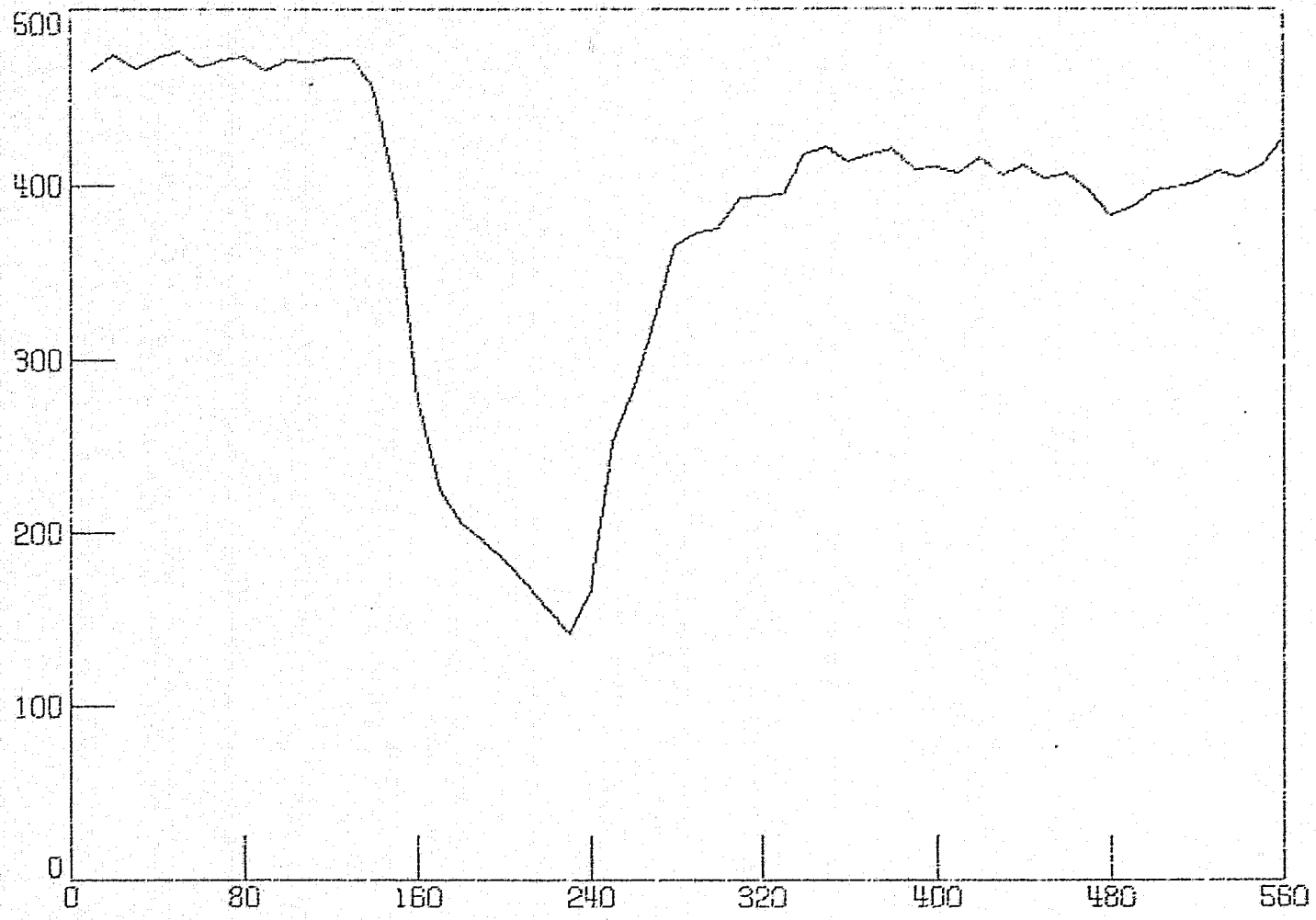

Figure 2. File B: Number of Background Water Pixels vs. Column Number.

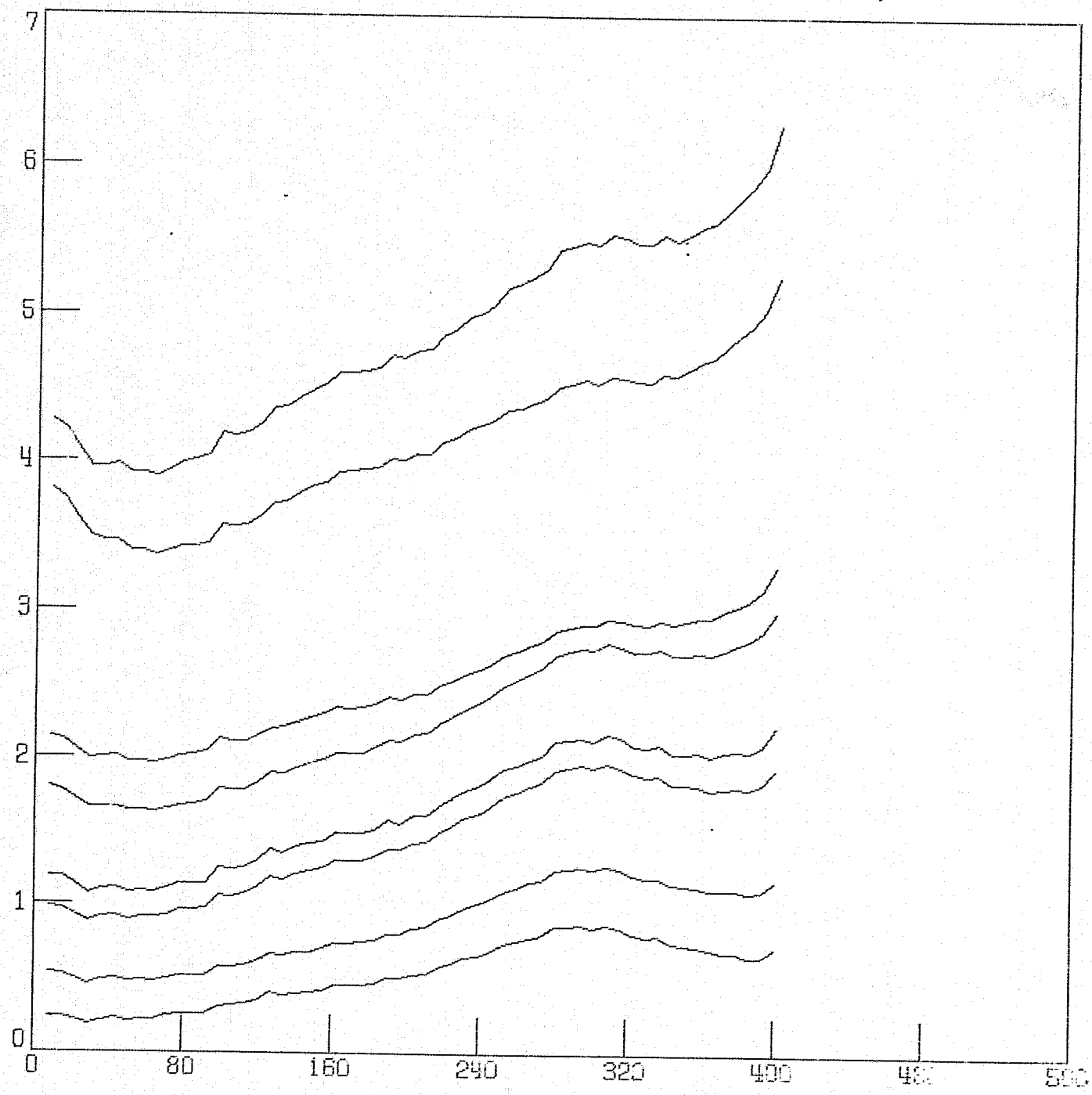

Figure 3. File A: Background Water Average Radiances vs. Column Number.

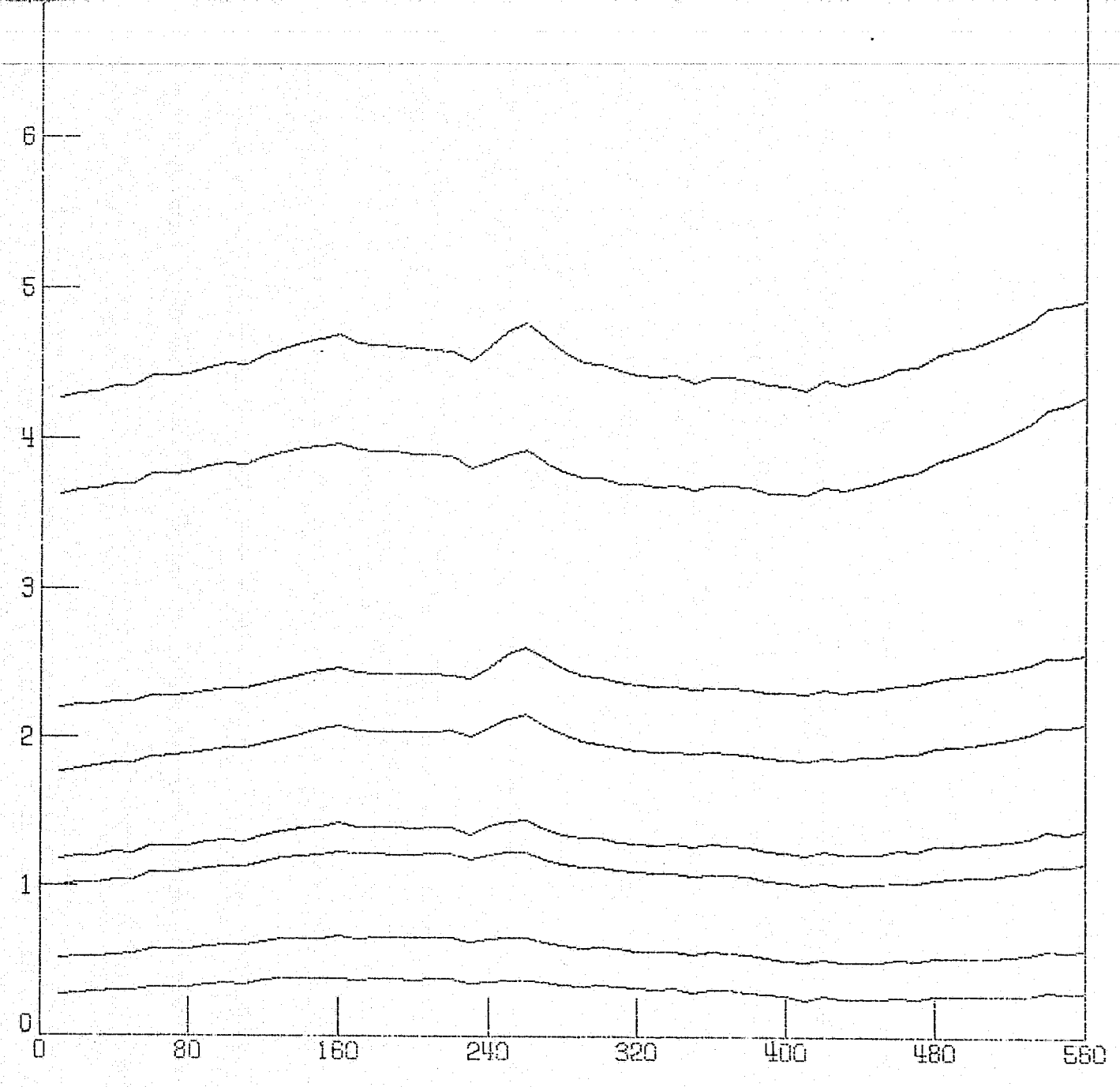

Figure 4. File B: Background Water Average Radiances vs. Column Number.

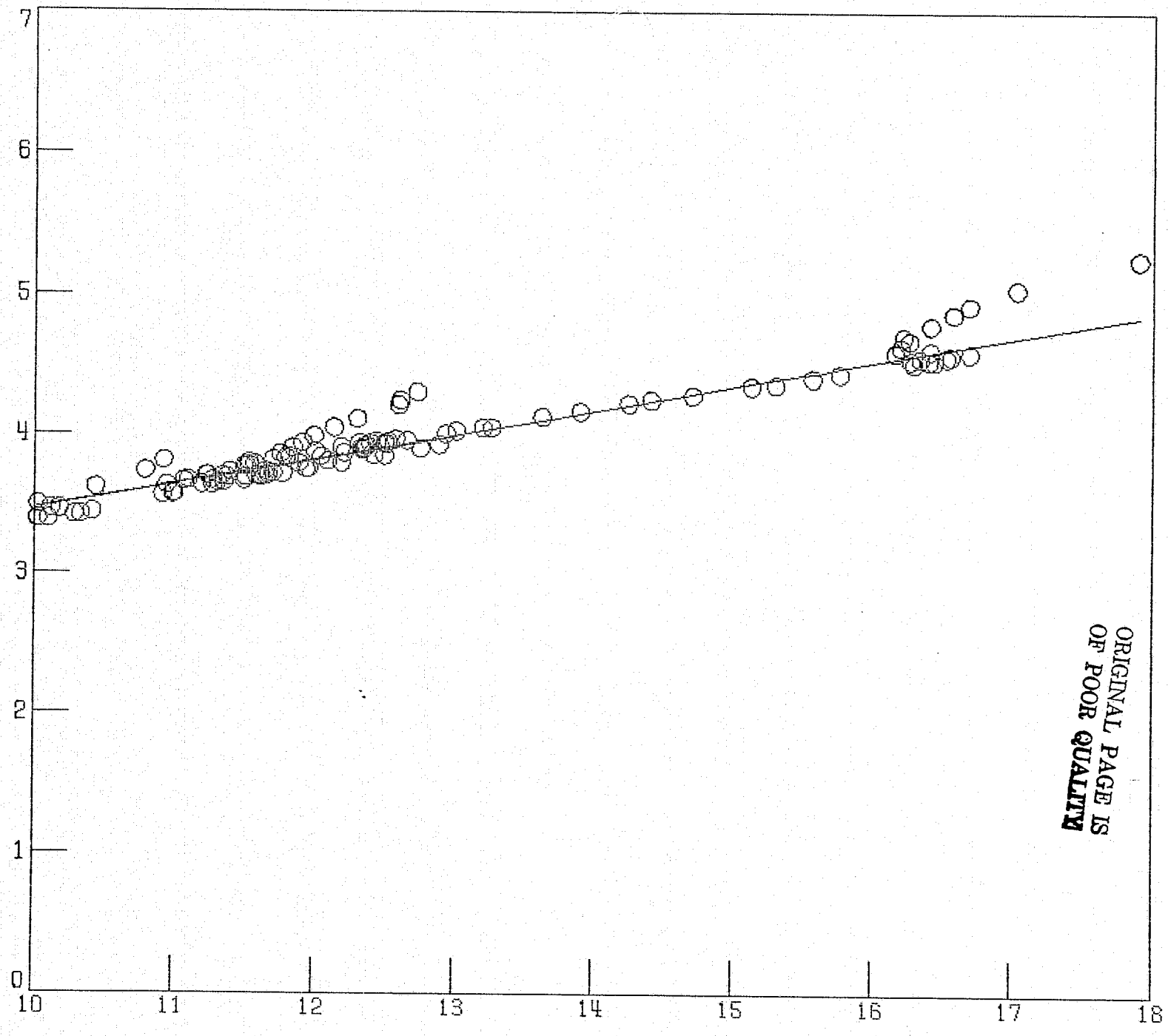

Figure 5. Channel 2 Average Radiance for Background Water vs. Σ

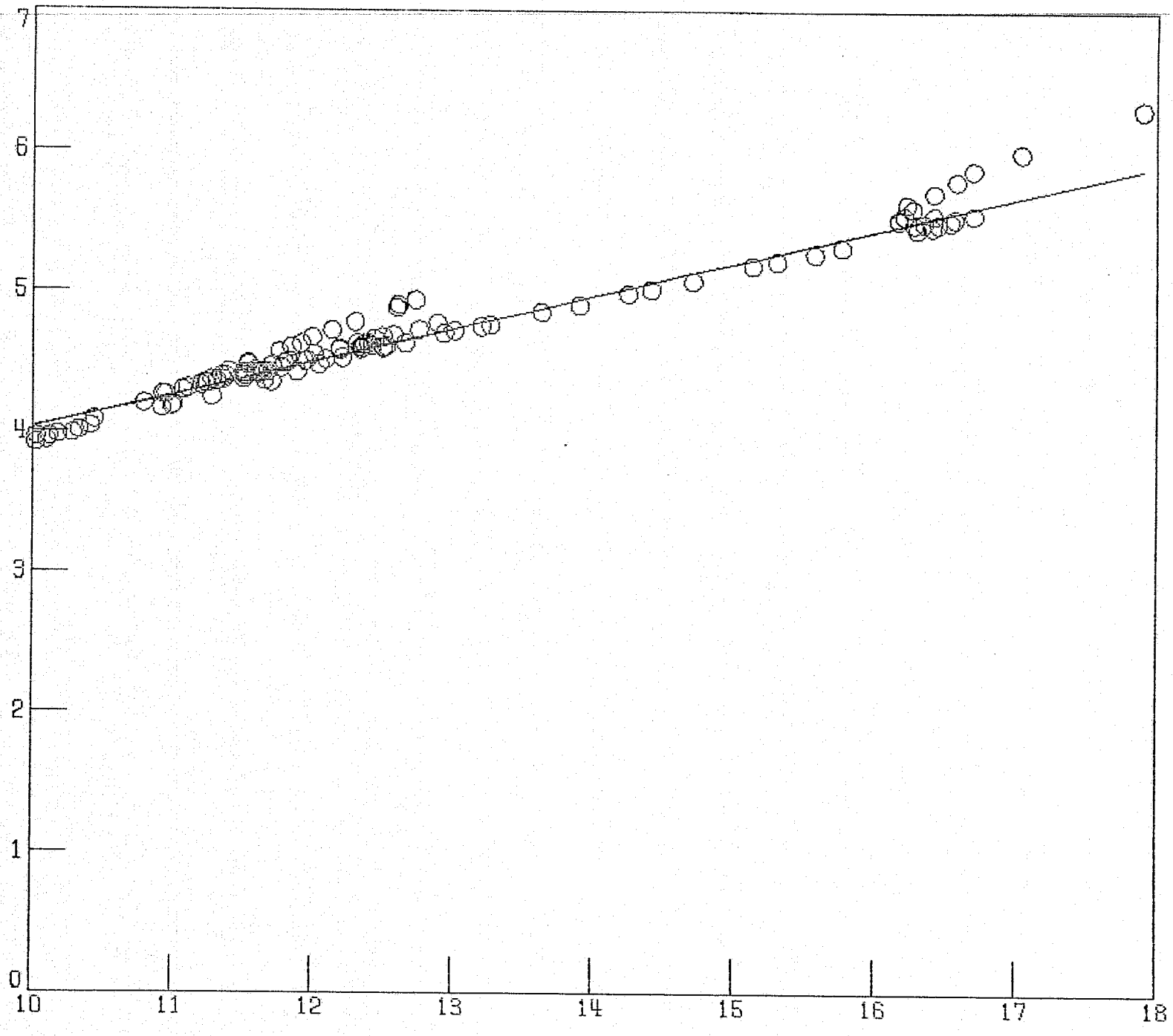

Figure 6. Channel 3 Average Radiance for Background Water vs. Σ

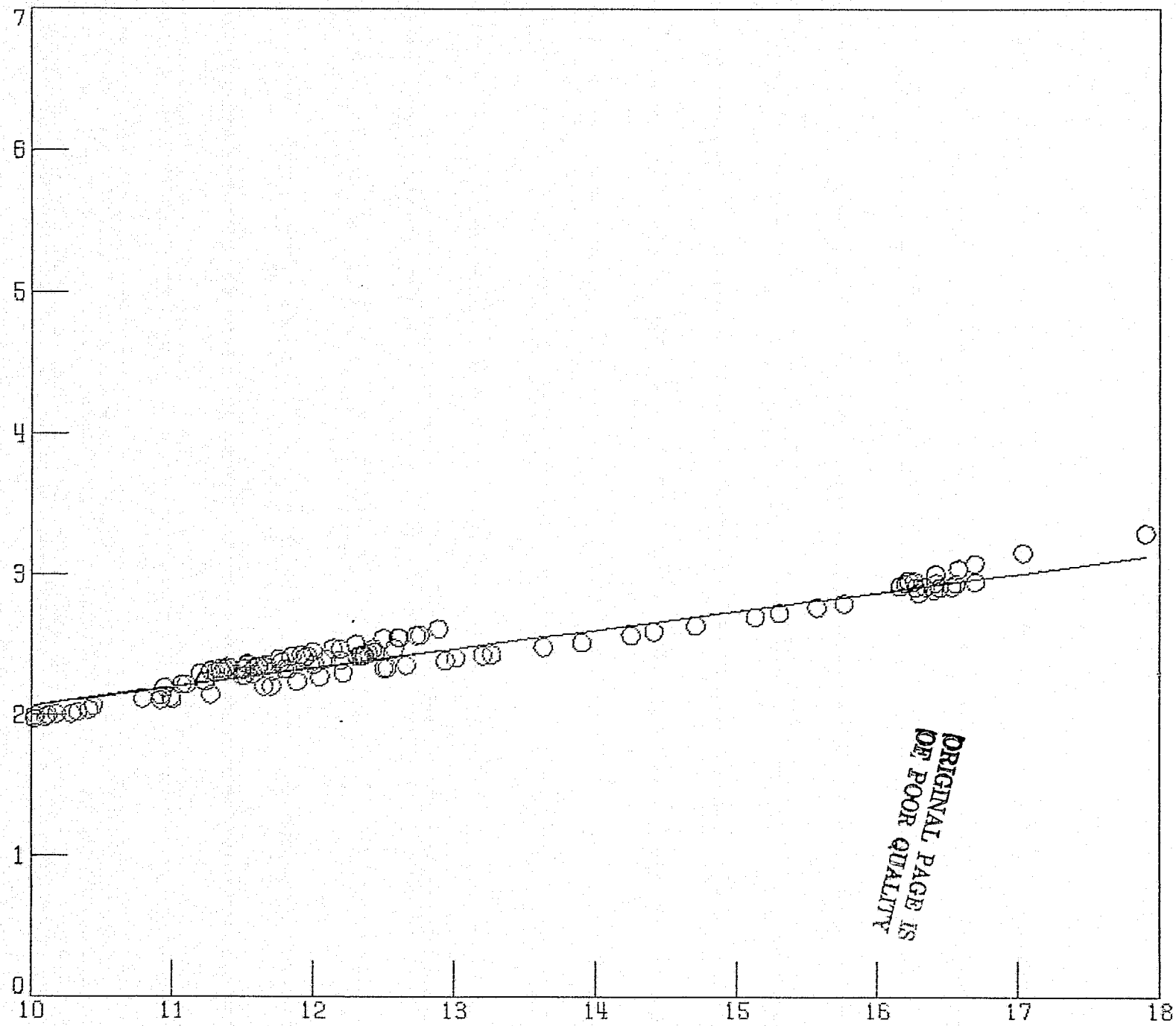

Figure 7. Channel 4 Average Radiance for Background Water vs. Σ

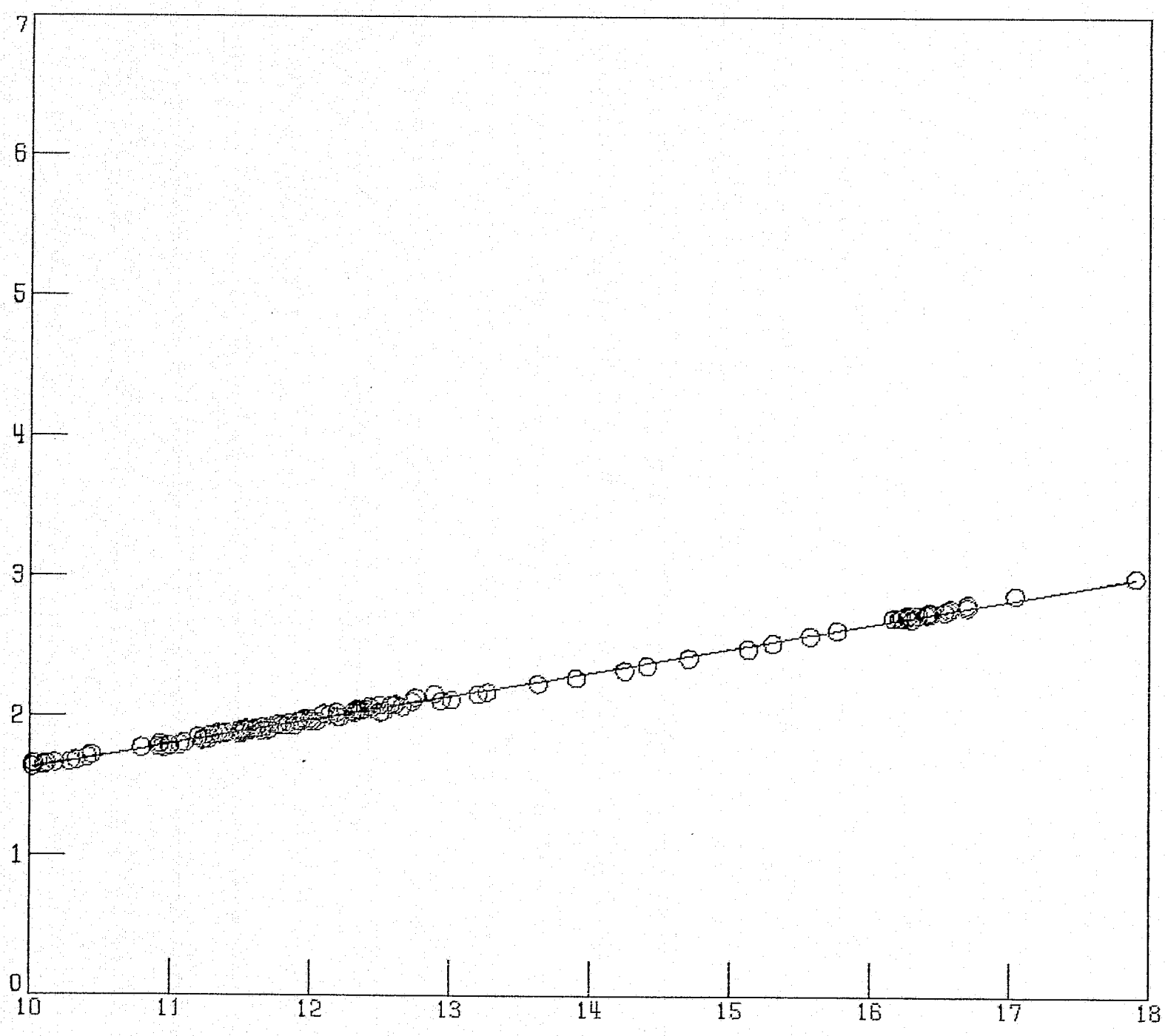

Figure 8. Channel 5 Average Radiance for Background Water vs. Σ

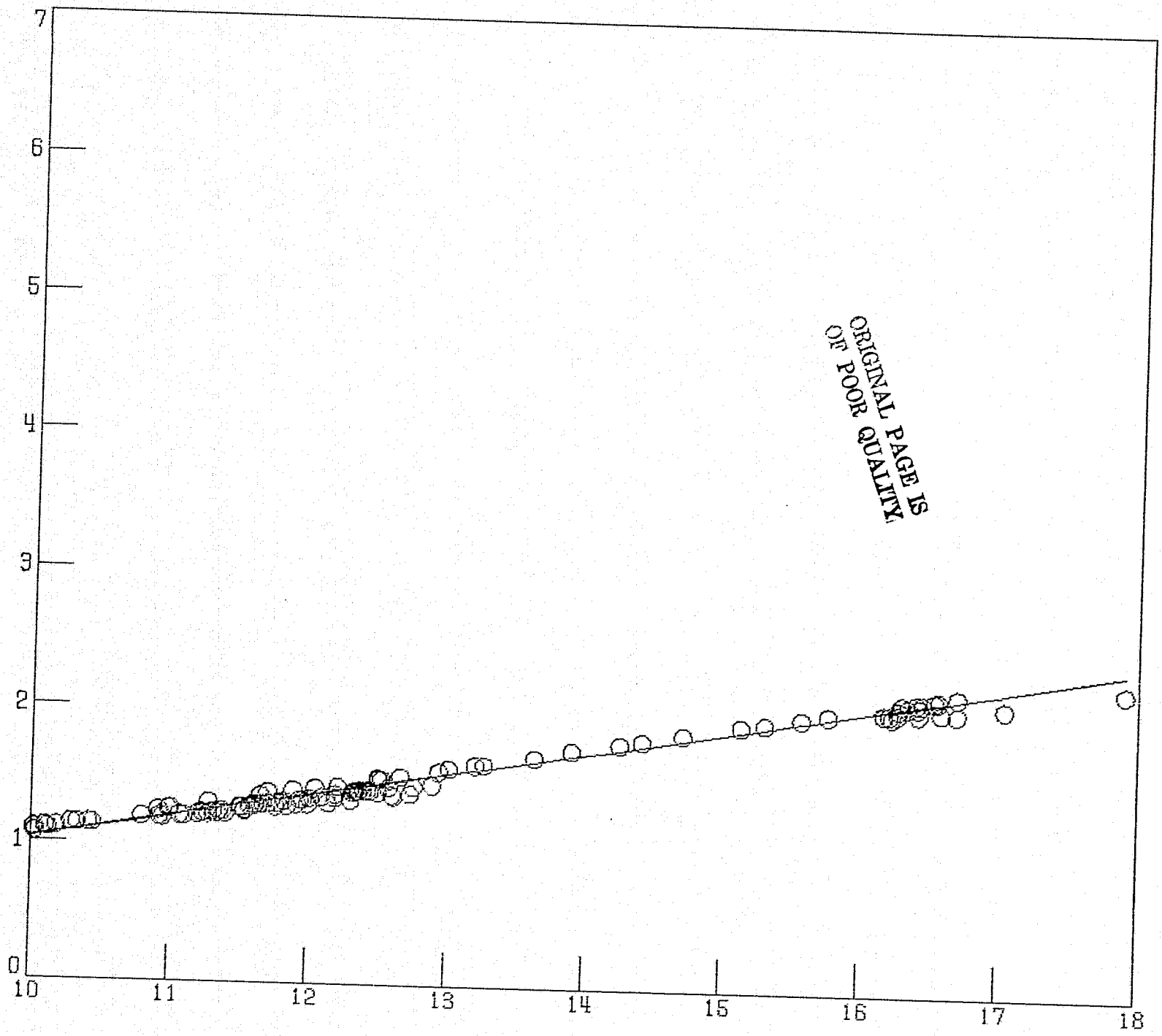

Figure 9. Channel 6 Average Radiance for Background Water vs. Σ

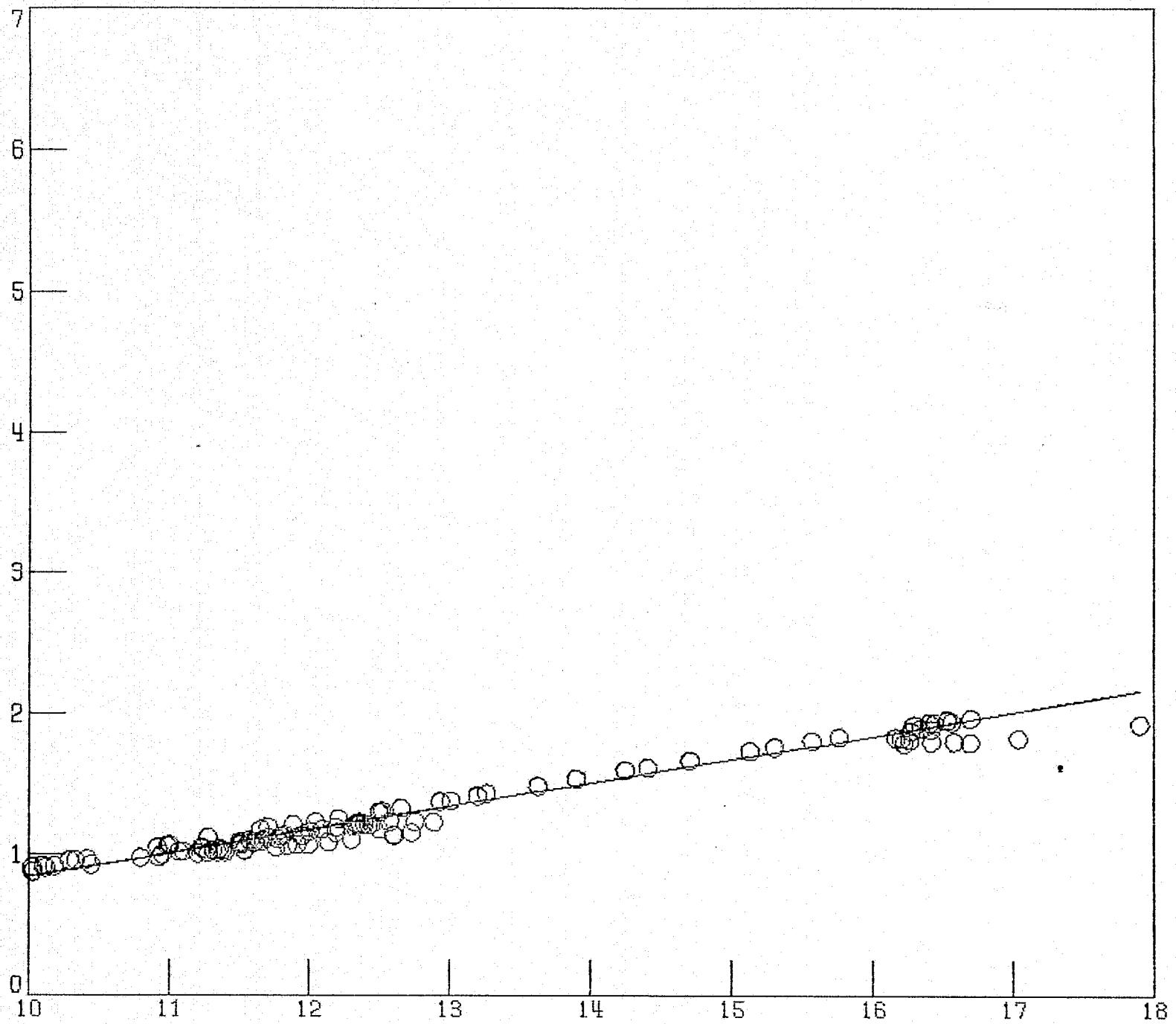

Figure 10. Channel 7 Average Radiance for Background Water vs. Σ

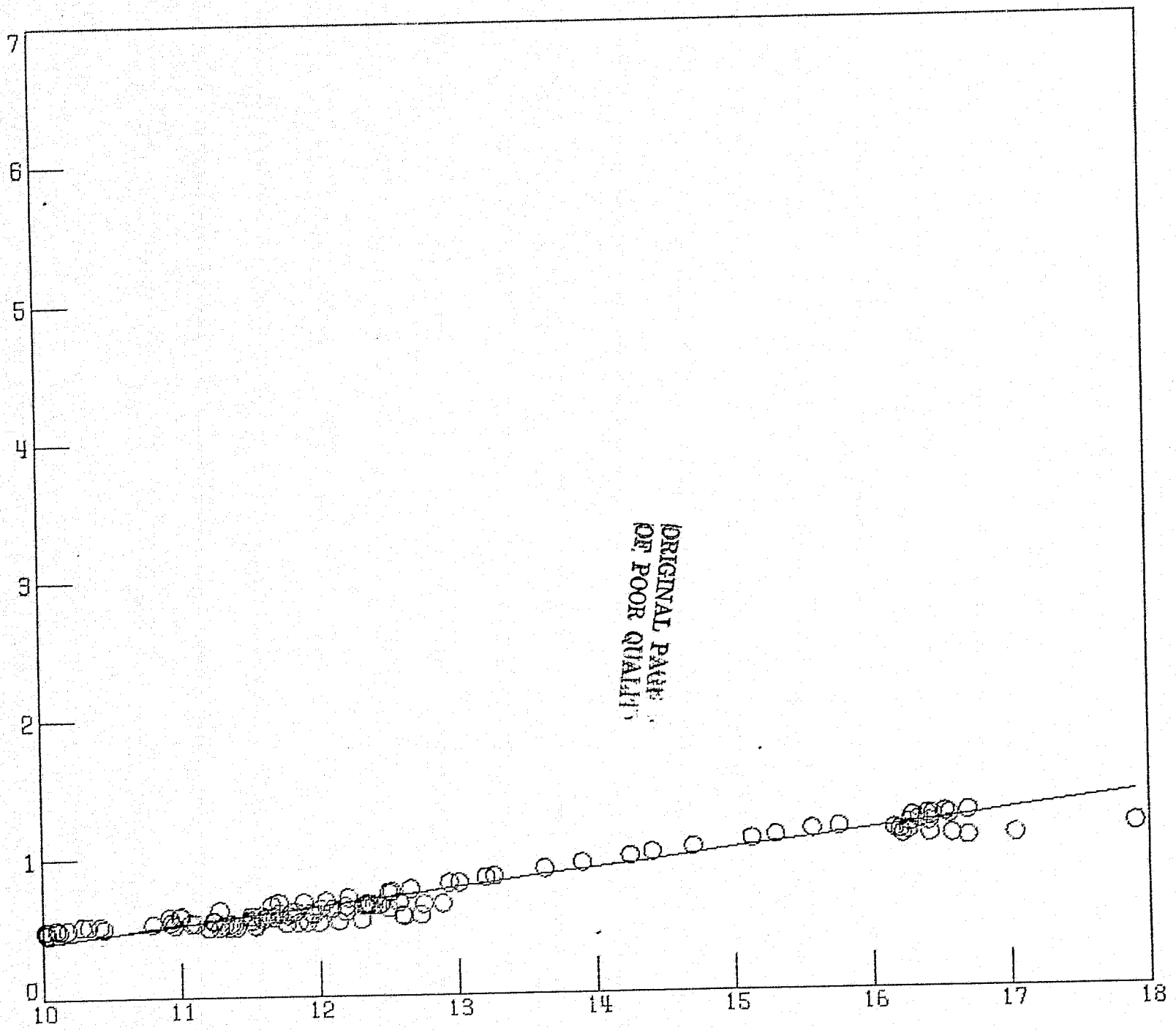

Figure 11. Channel 8 Average Radiance for Background Water vs. Σ

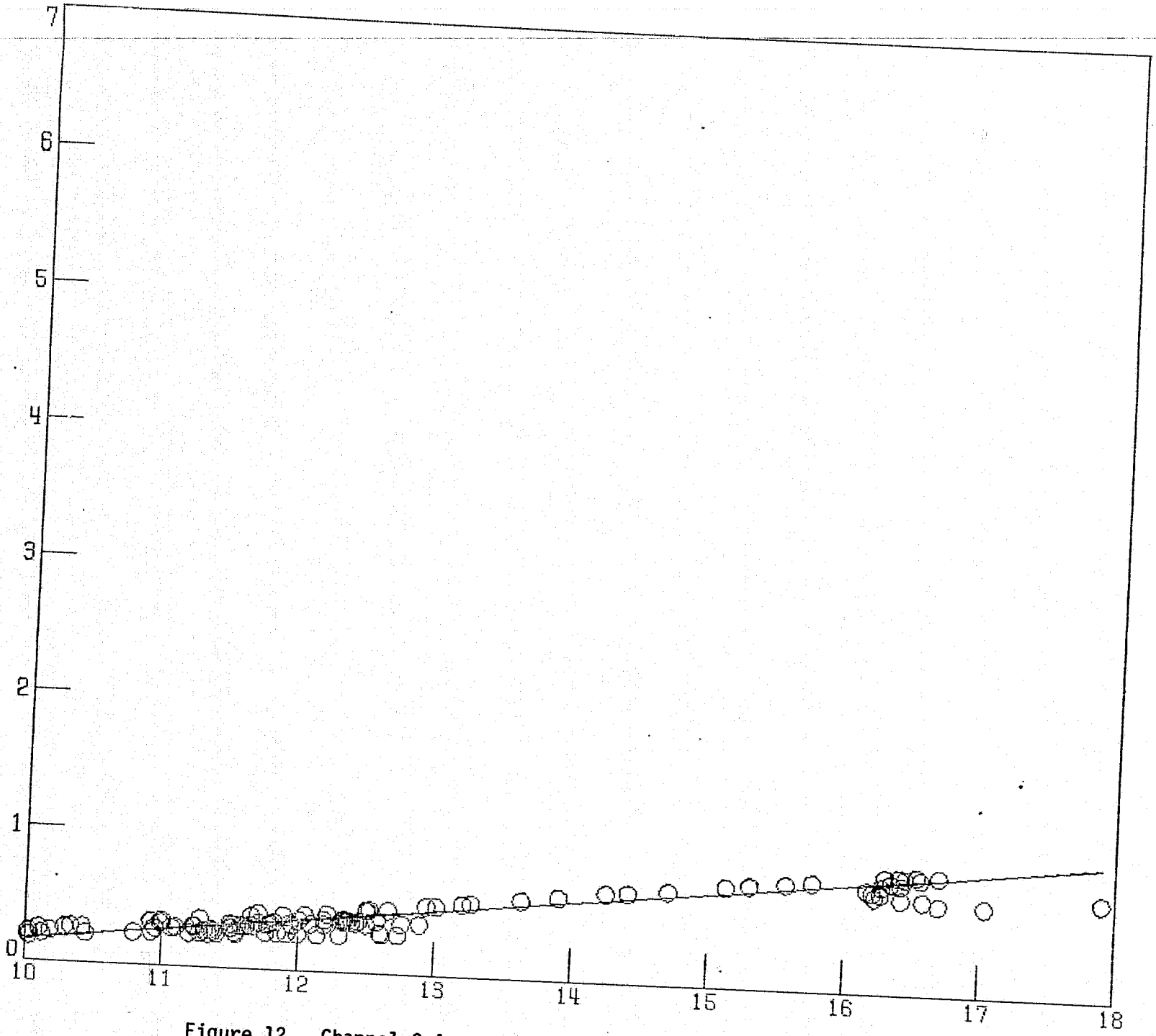

Figure 12. Channel 9 Average Radiance for Background Water vs. Σ

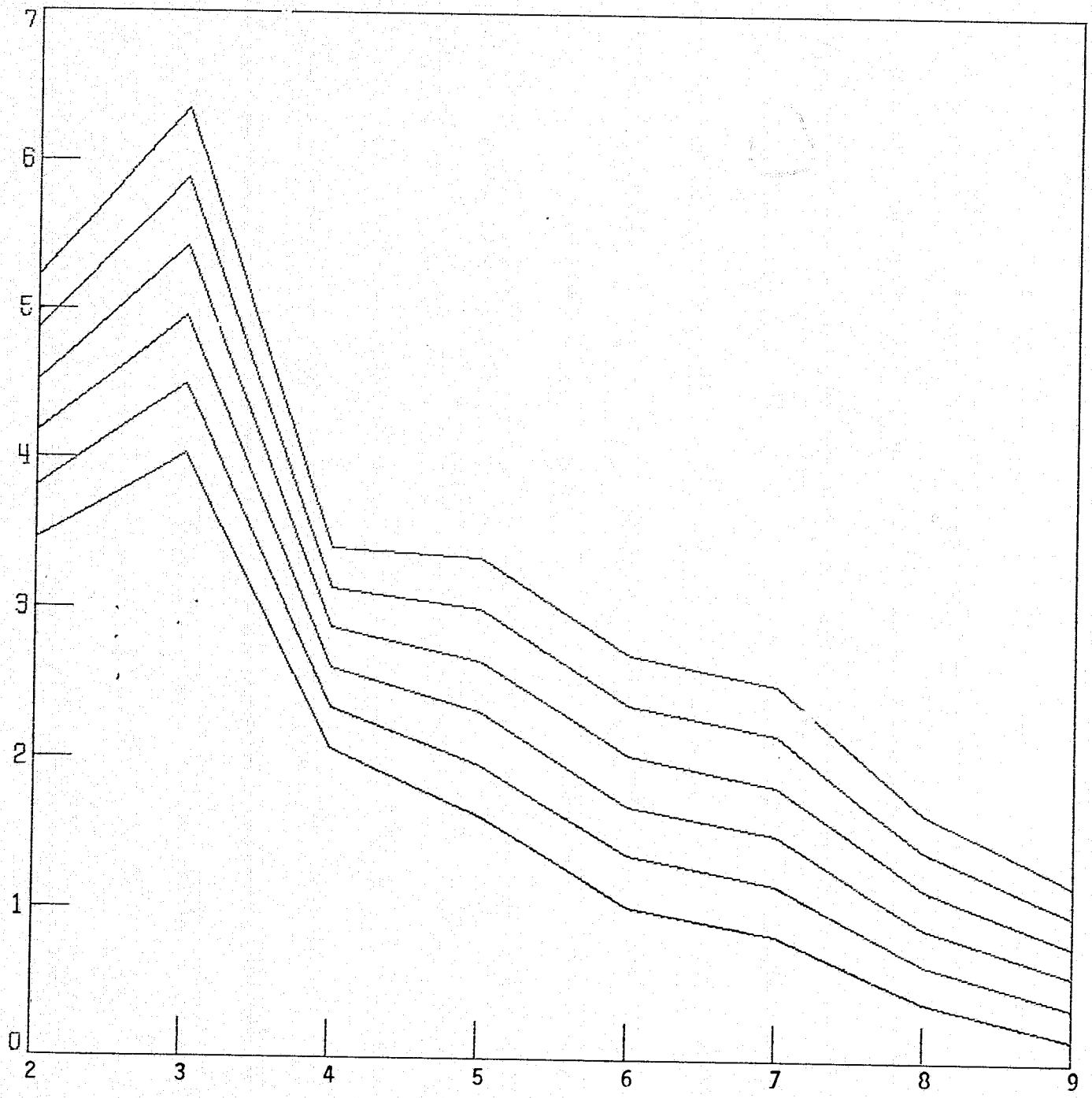

Figure 13. Background Water Radiances for Various Sunlight Intensities (10, 12, 14, 16, 18, and 20 Values for Σ) vs. Channel Number

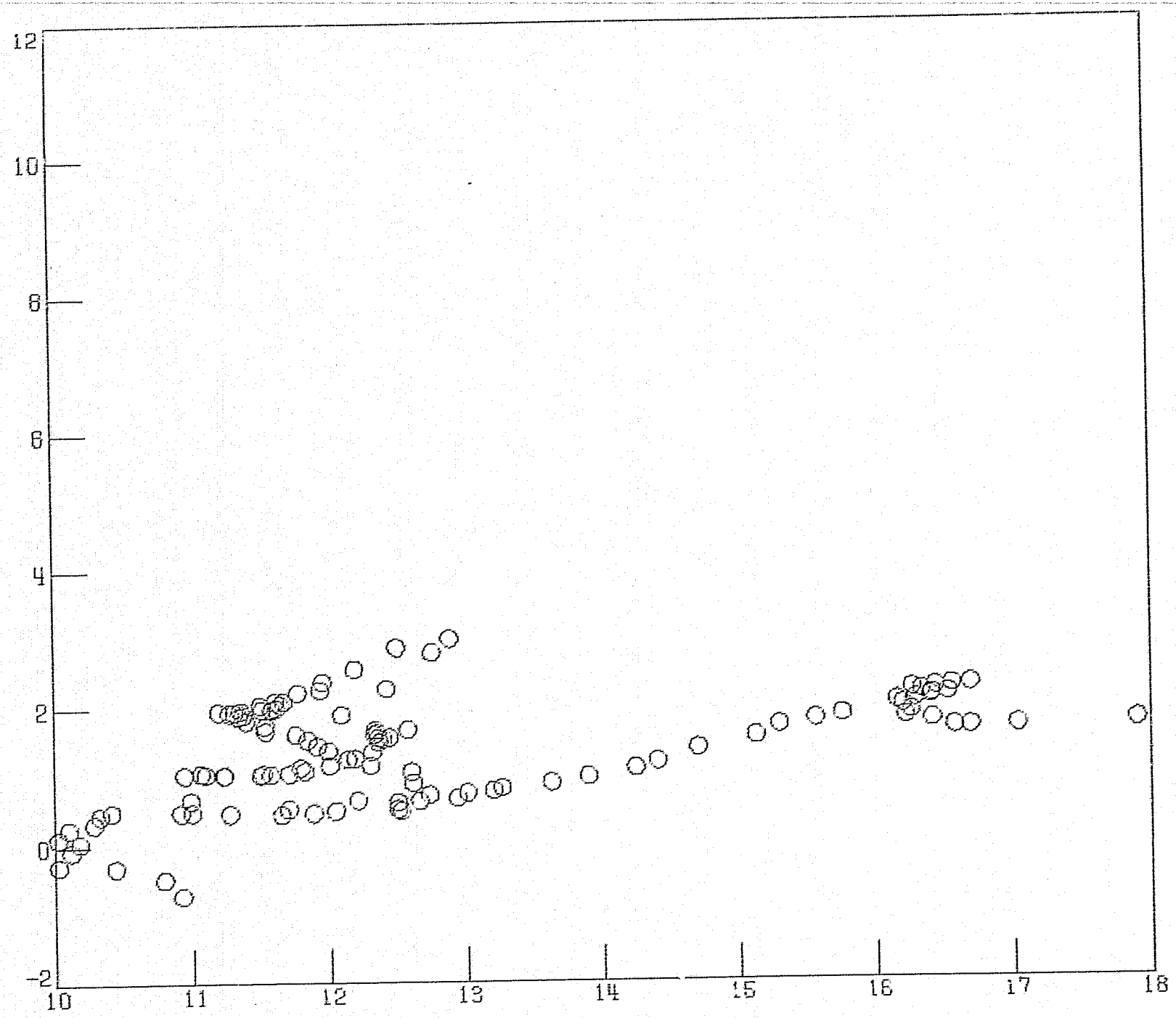

Figure 14. Calculated Values of Iron Concentration for Background Water Data vs. Σ

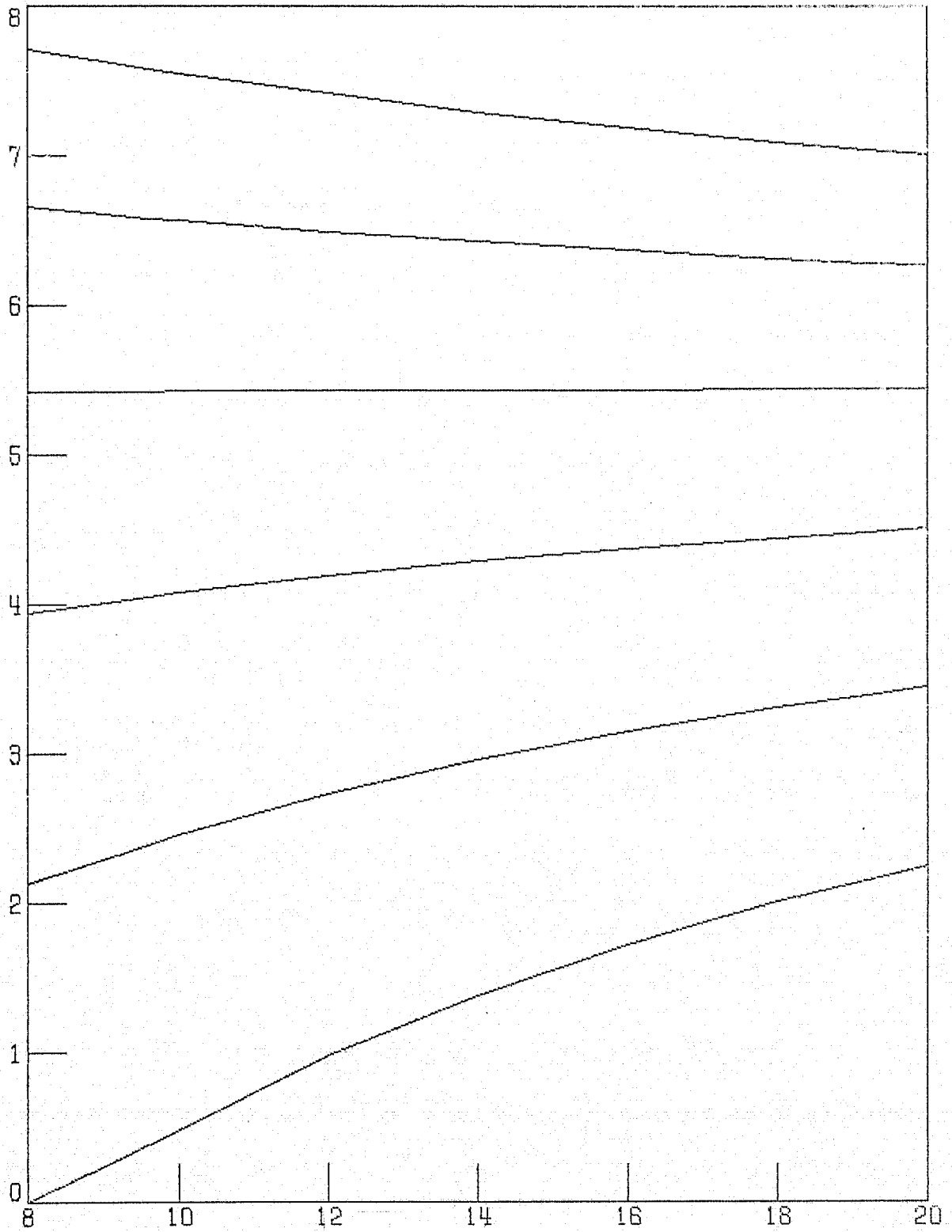

Figure 15. Calculated Iron Concentration as a Function of Sunglitter, Showing the Effect of Sunglitter (as Measured by Σ) at Various Levels of Actual Iron Concentration

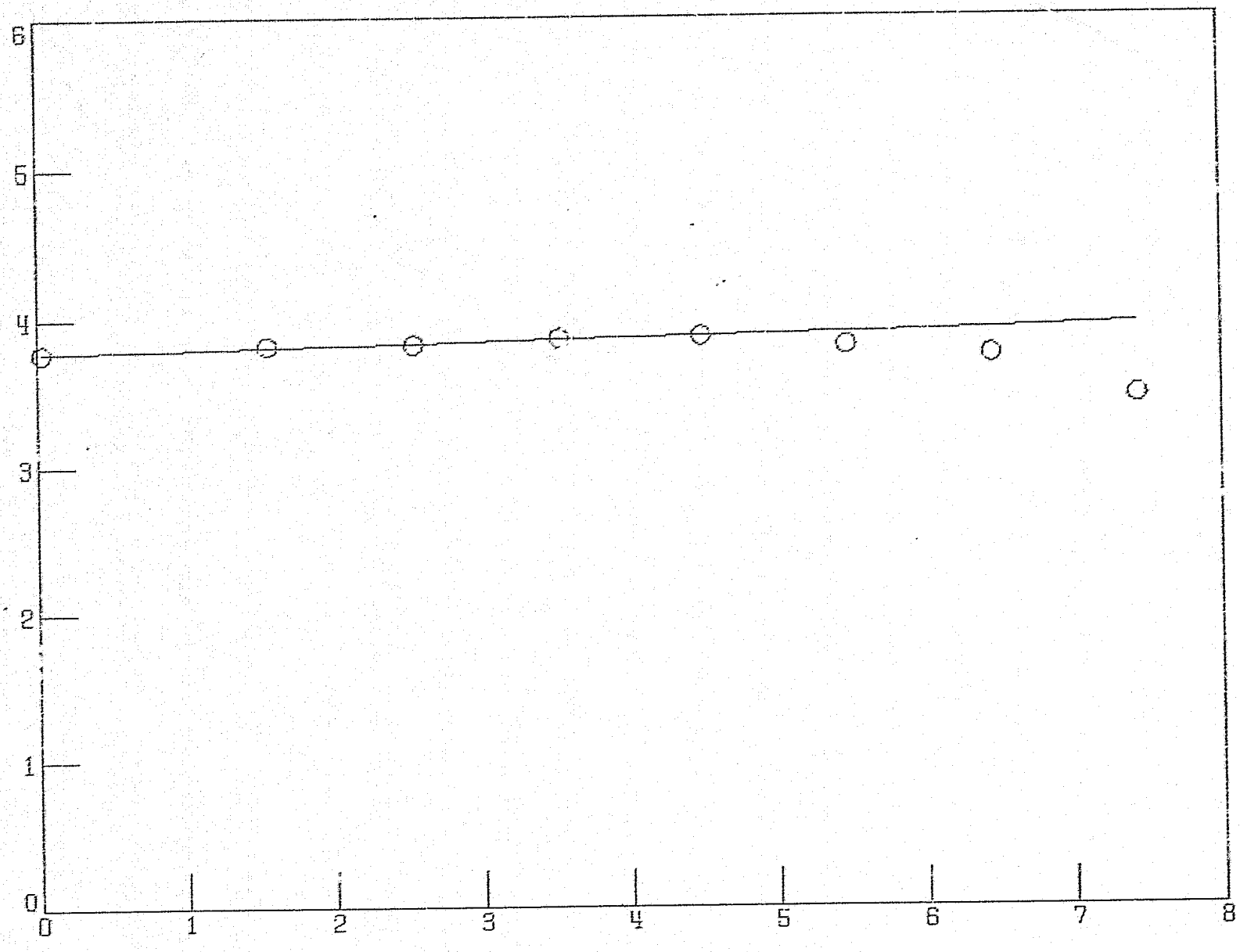

Figure 16. Channel 2: Adjusted Radiance vs. Iron Concentration

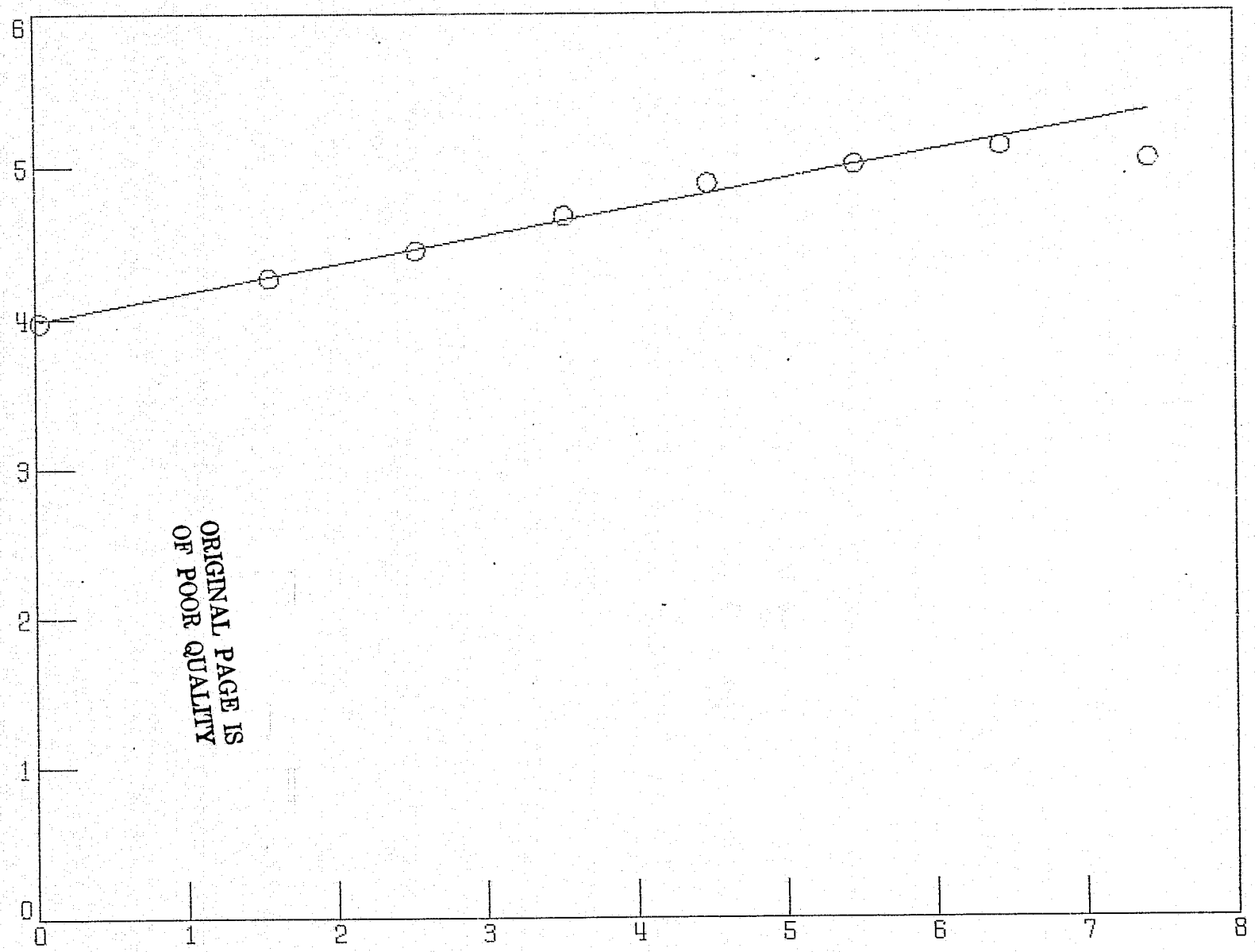

Figure 17. Channel 3: Adjusted Radiance vs. Iron Concentration

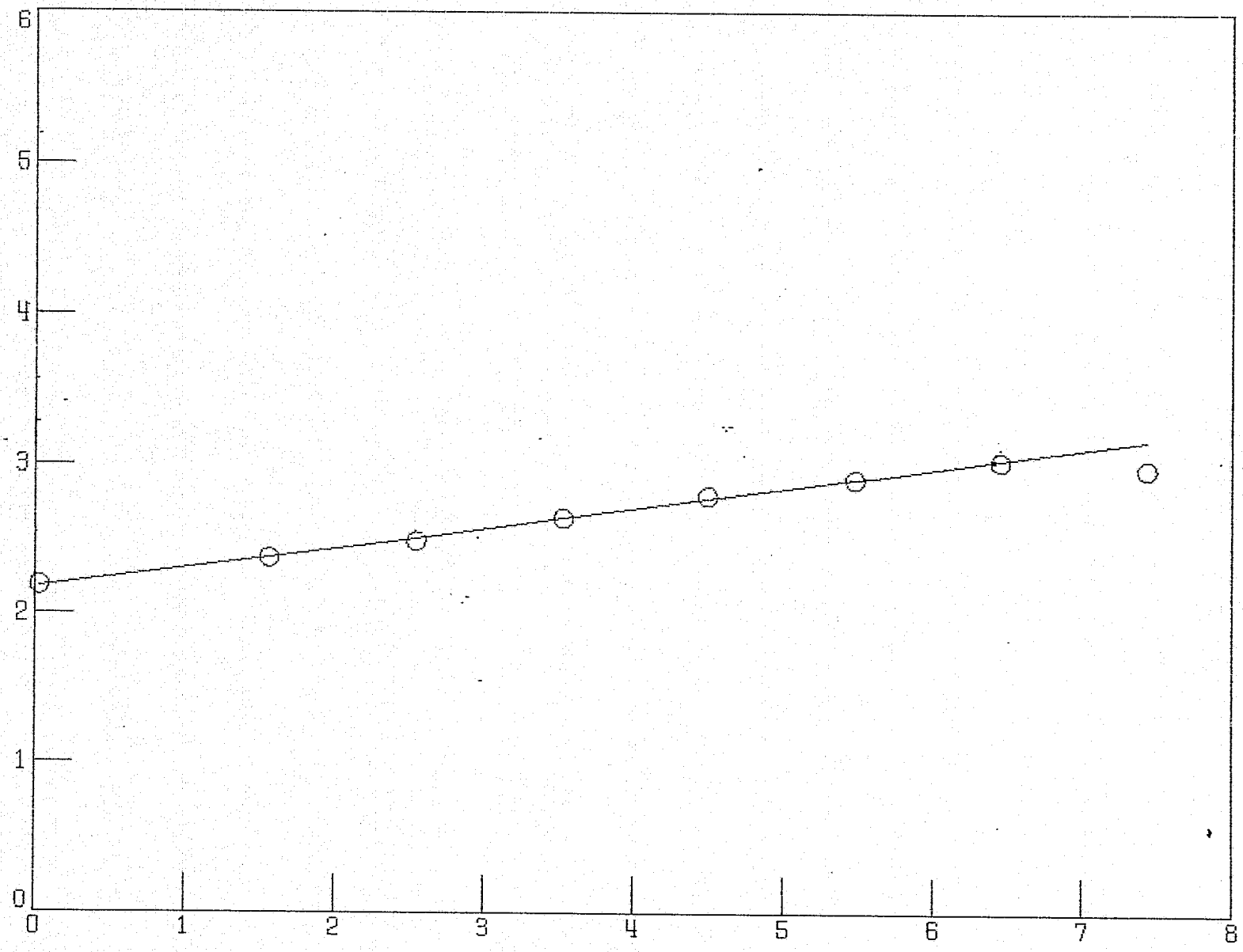

Figure 18. Channel 4: Adjusted Radiance vs. Iron Concentration

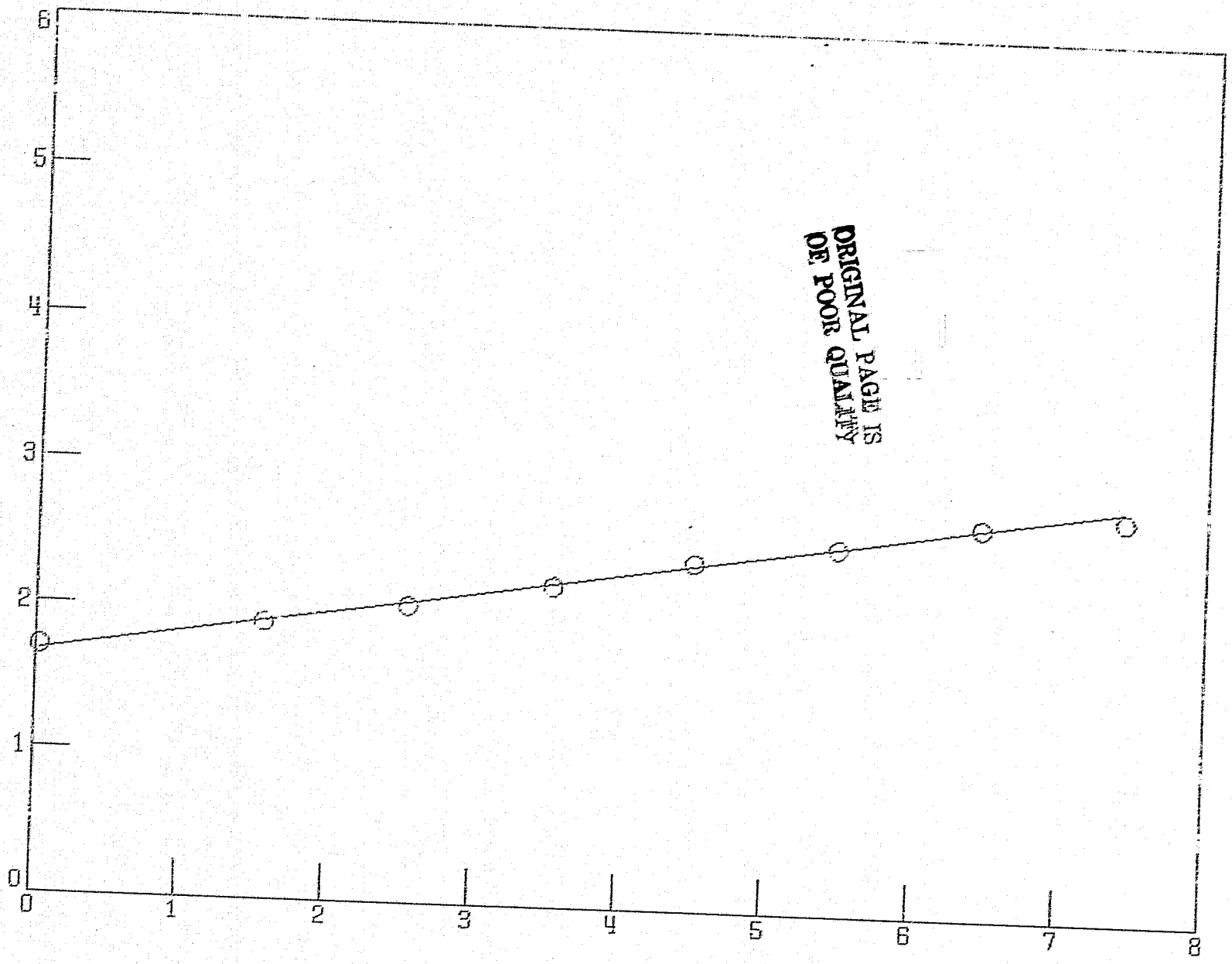

Figure 19. Channel 5: Adjusted Radiance vs. Iron Concentration

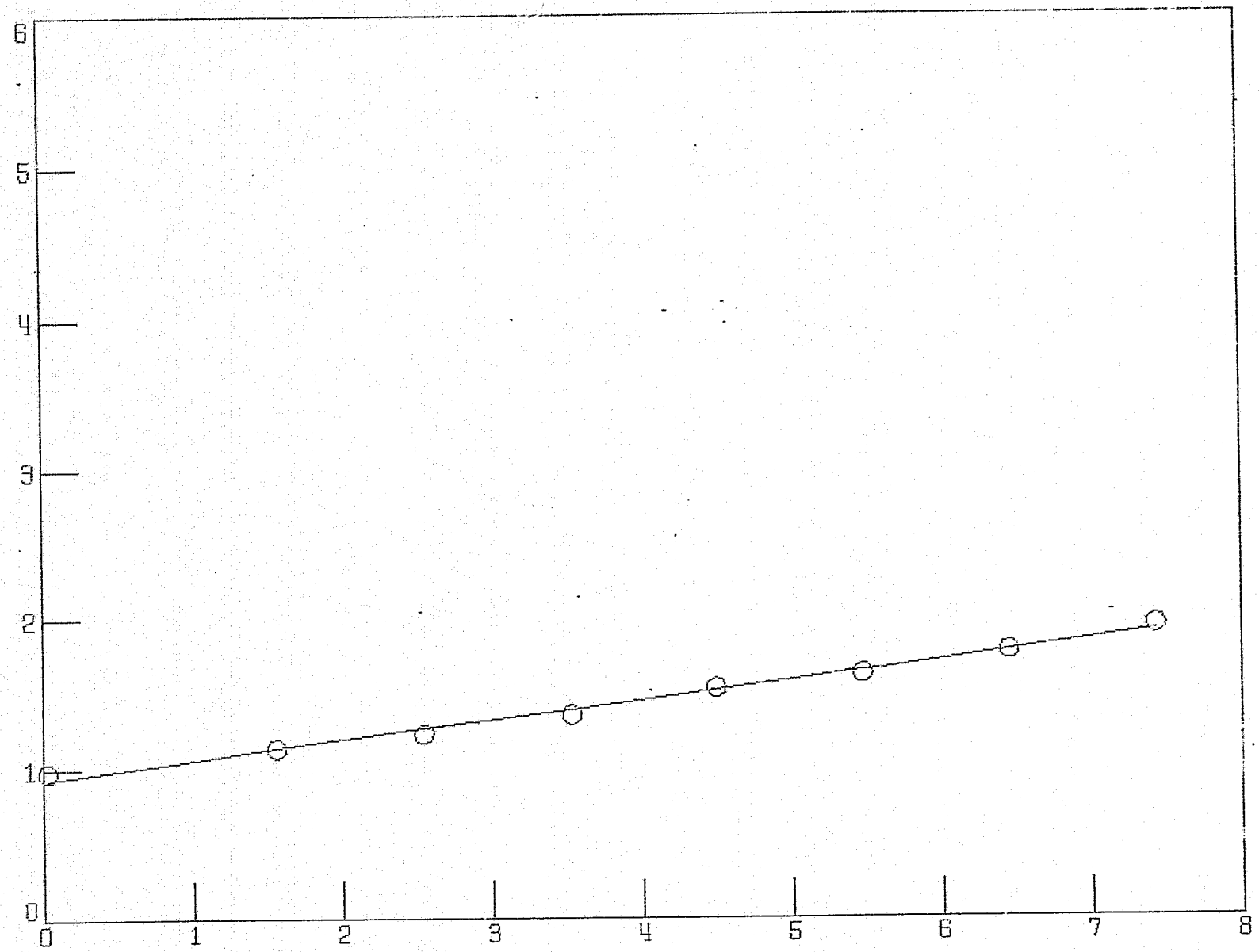

Figure 20. Channel 6: Adjusted Radiance vs. Iron Concentration

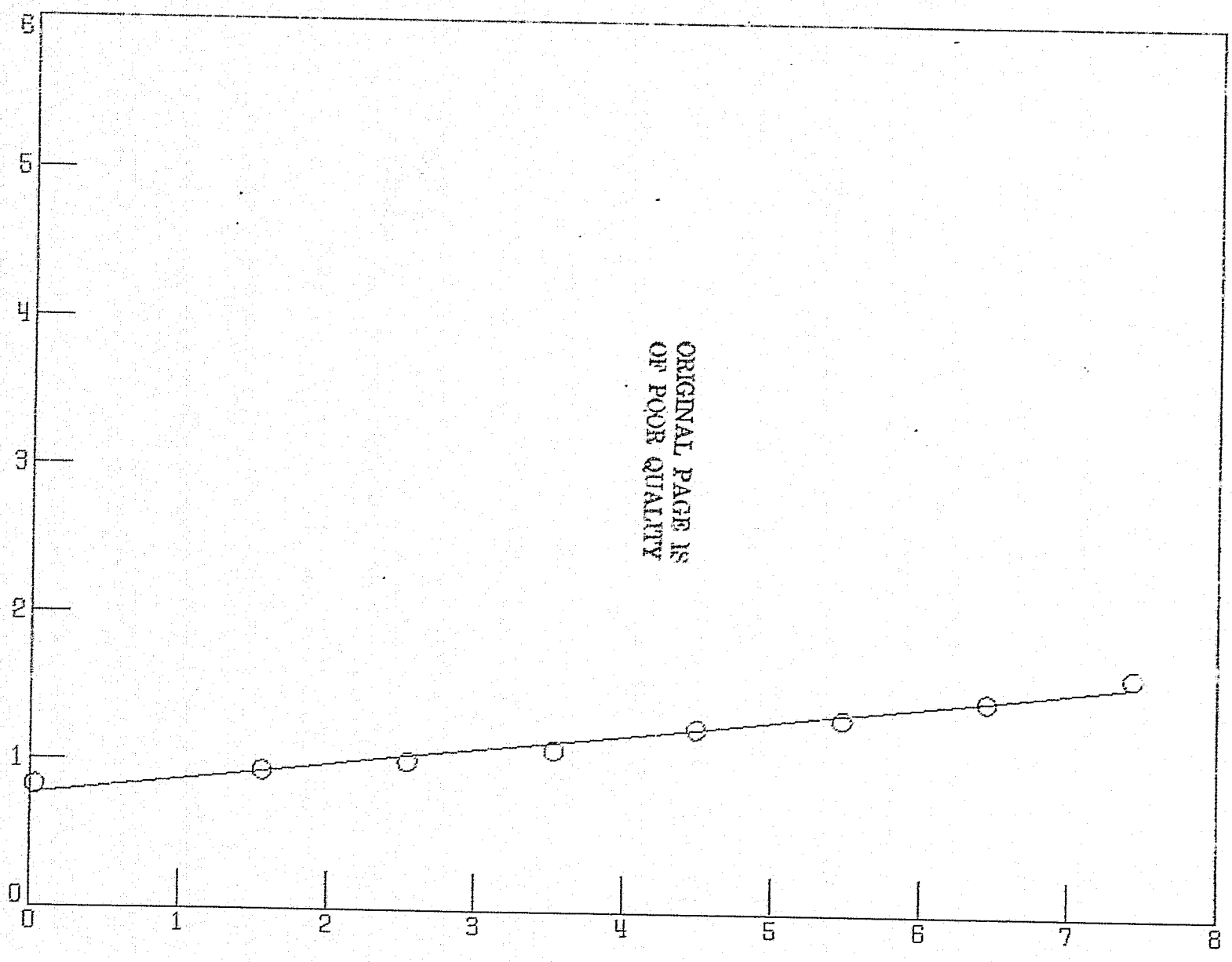

Figure 21. Channel 7: Adjusted Radiance vs. Iron Concentration

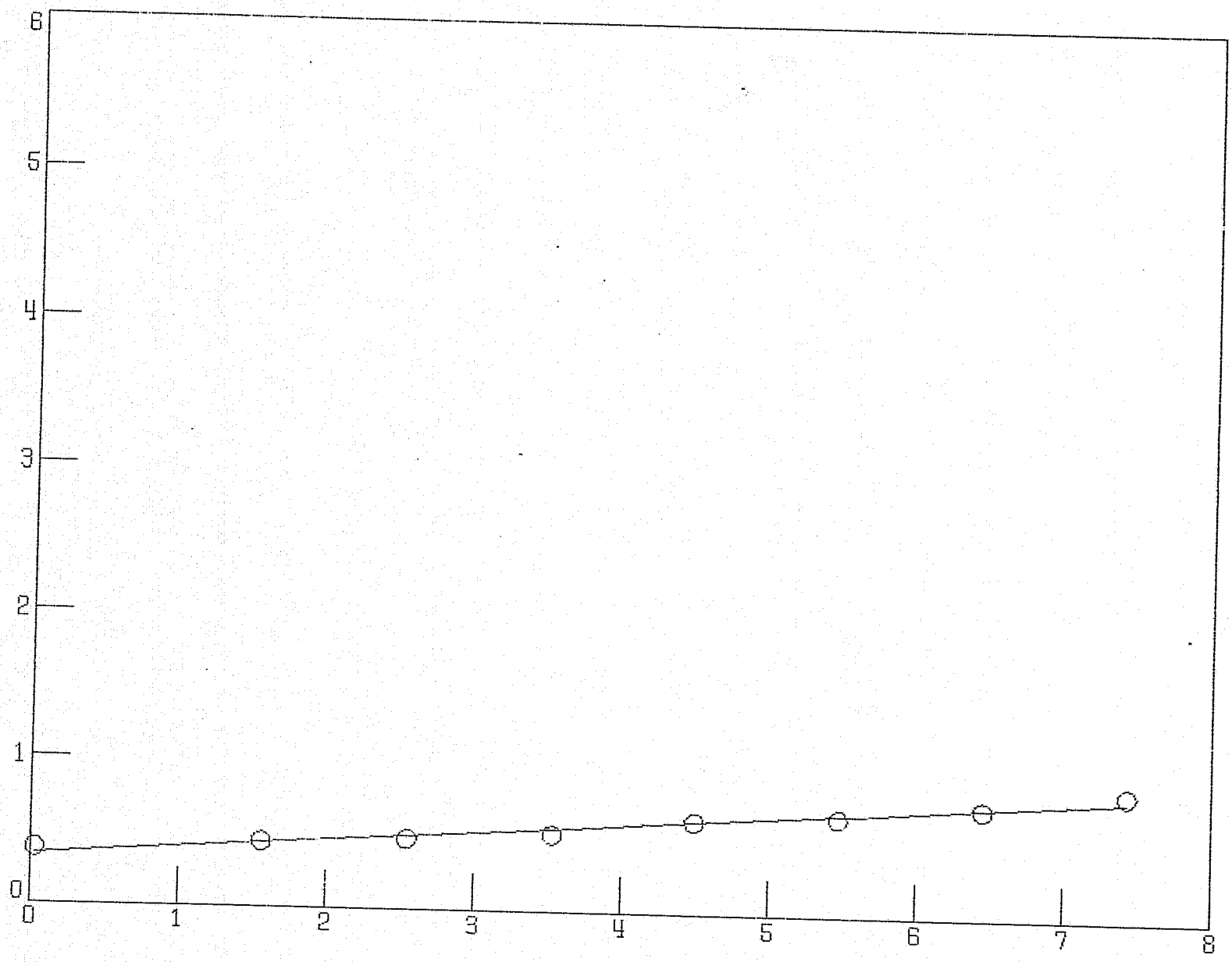

Figure 22. Channel 8: Adjusted Radiance vs. Iron Concentration

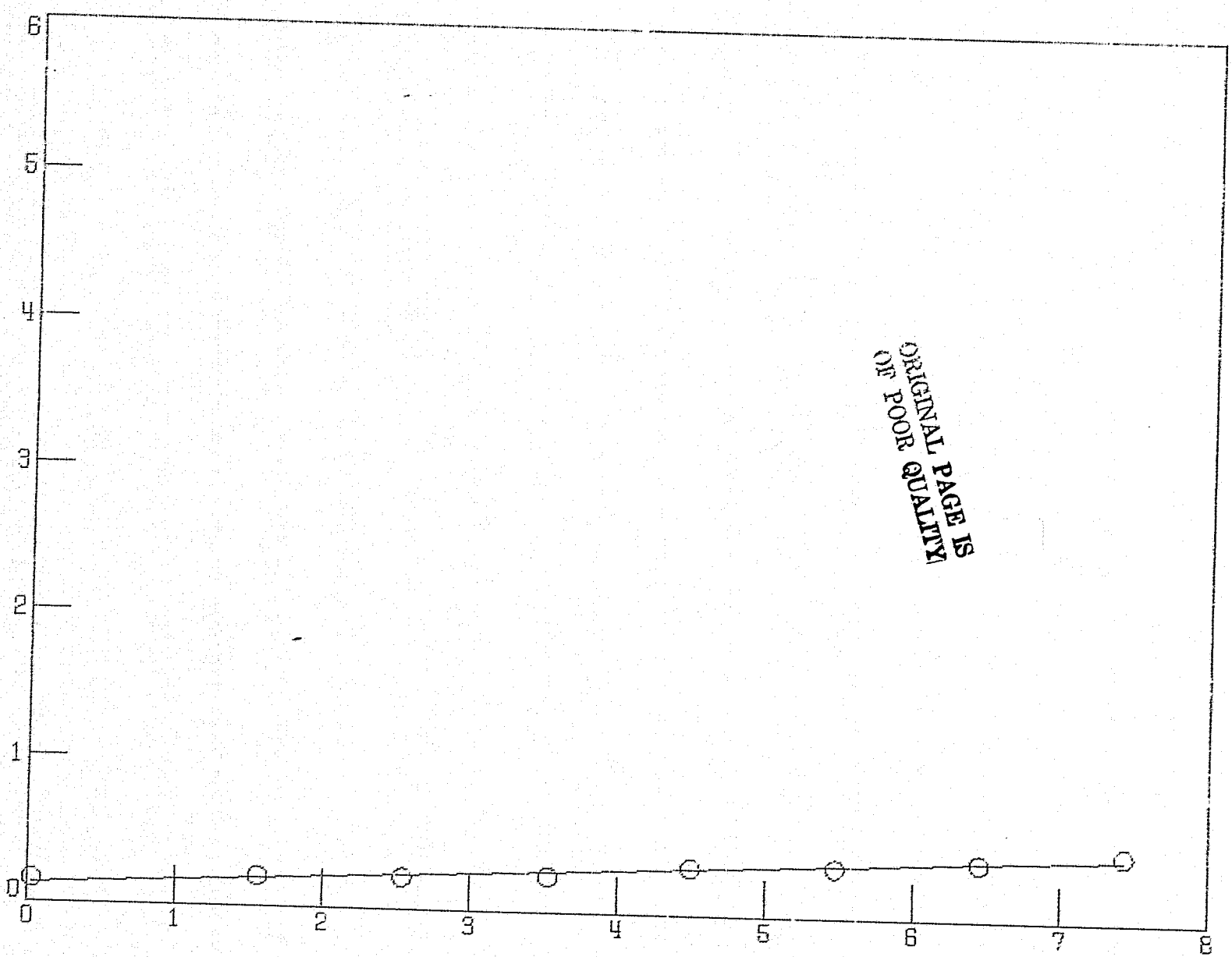

Figure 23. Channel 9: Adjusted Radiance vs. Iron Concentration

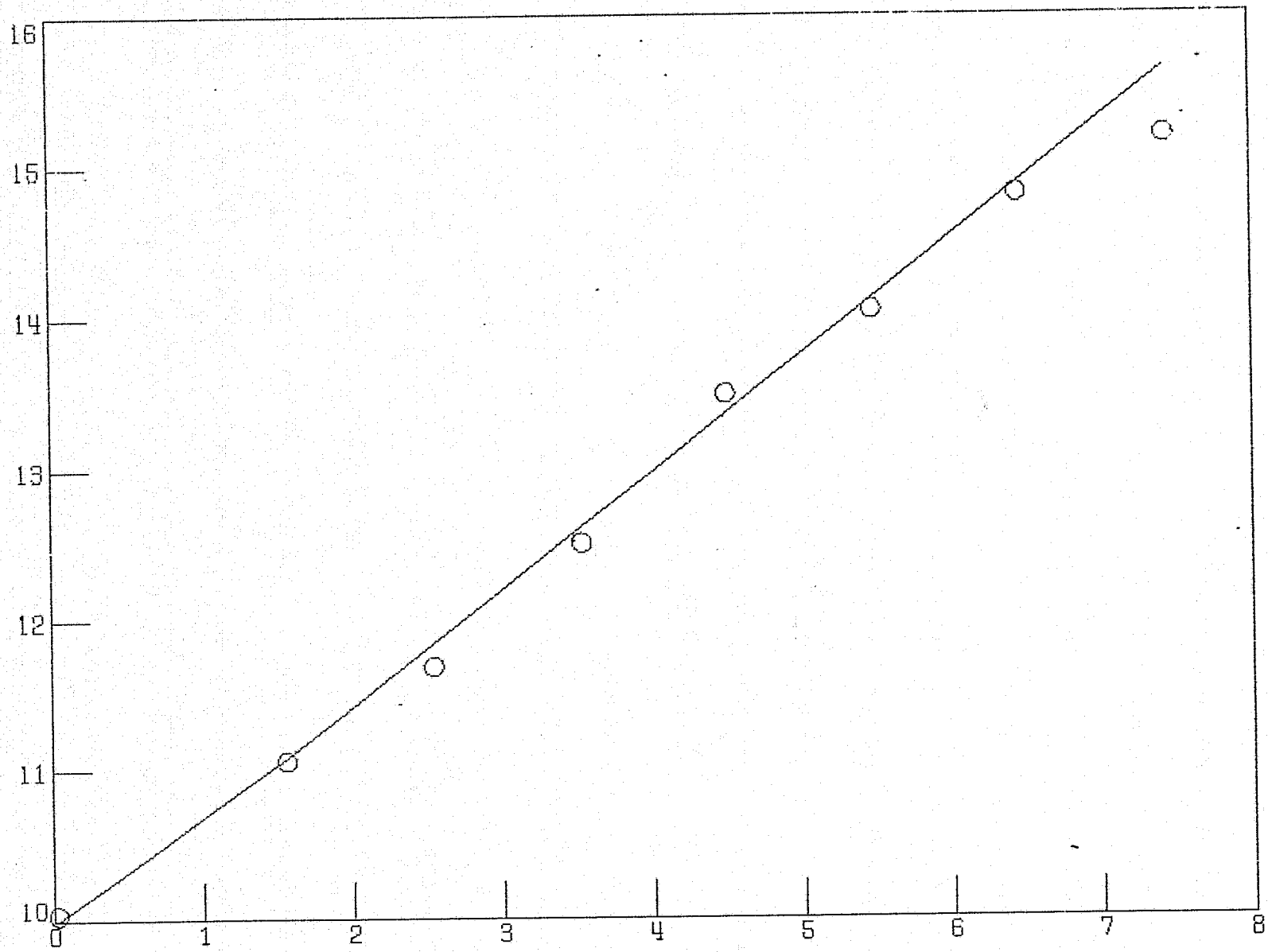

Figure 24. Σ for Adjusted Radiances of Channels 3-8 vs. Iron Concentration

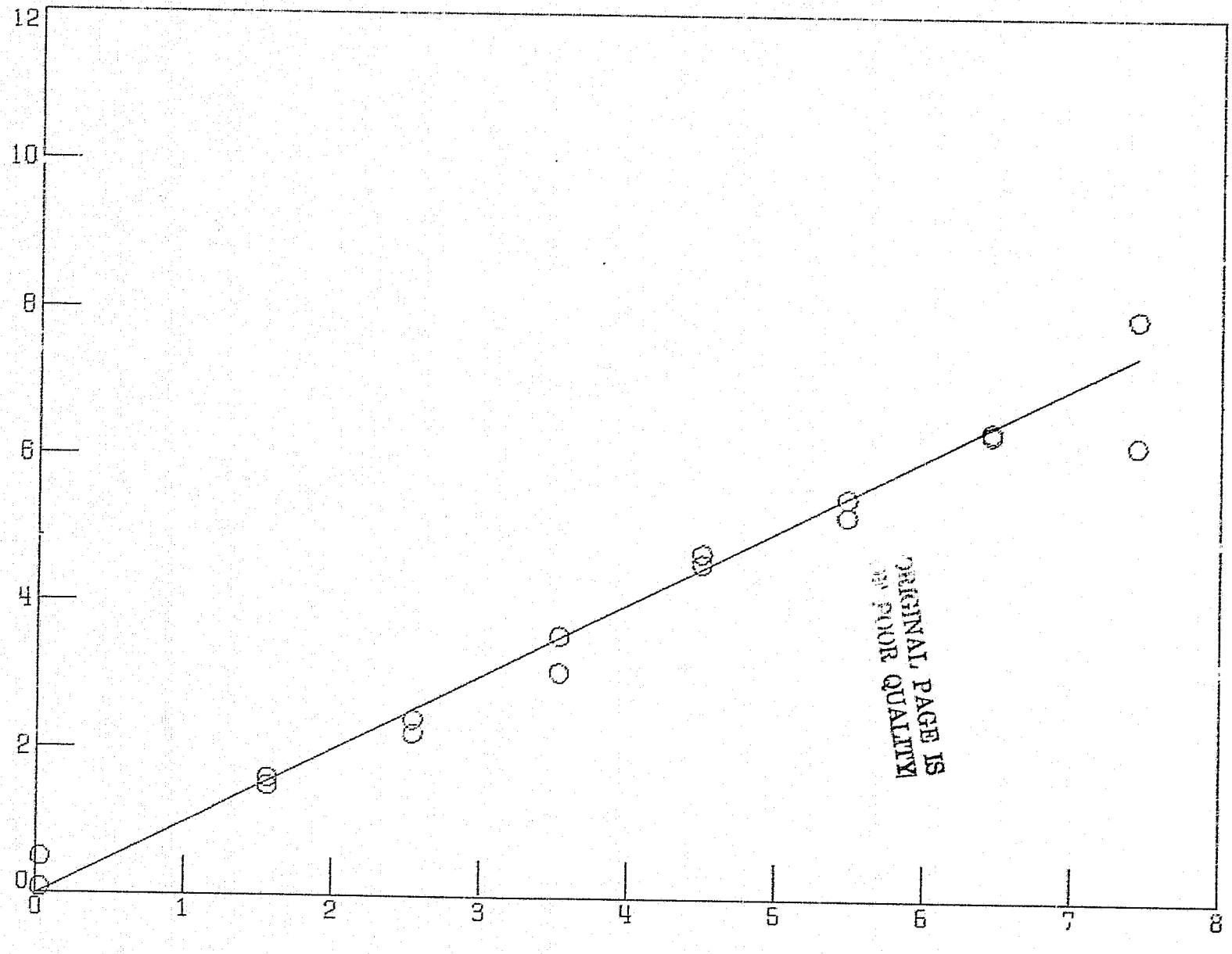

Figure 25. F_1 and F_2 Values for Iron Concentration vs. Original Equation Values

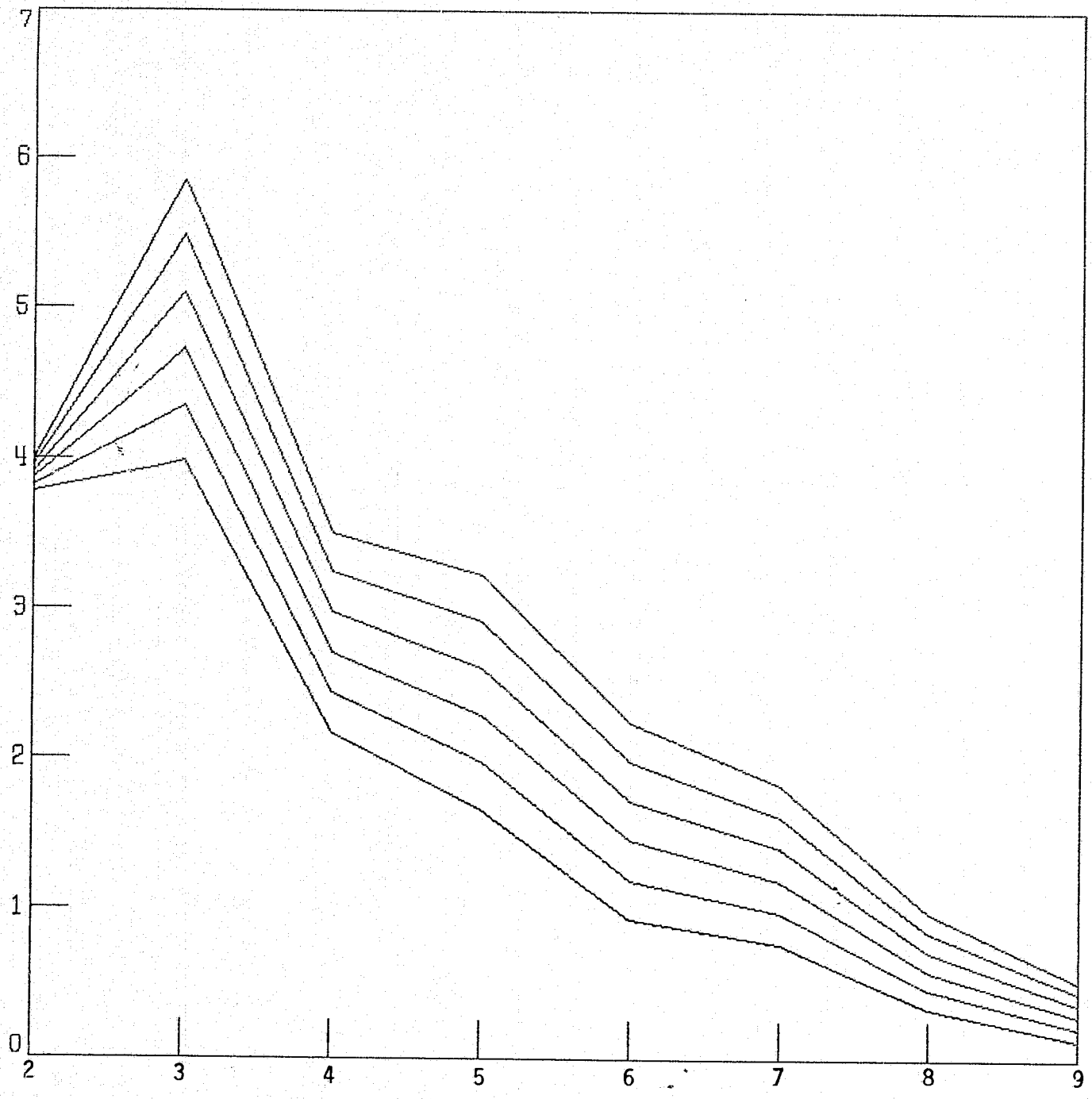

Figure 26. Dispersed Plume Radiances at Various Iron Concentrations (0, 2, 4, 6, 8, and 10 Nominal Values) vs. Channel Number

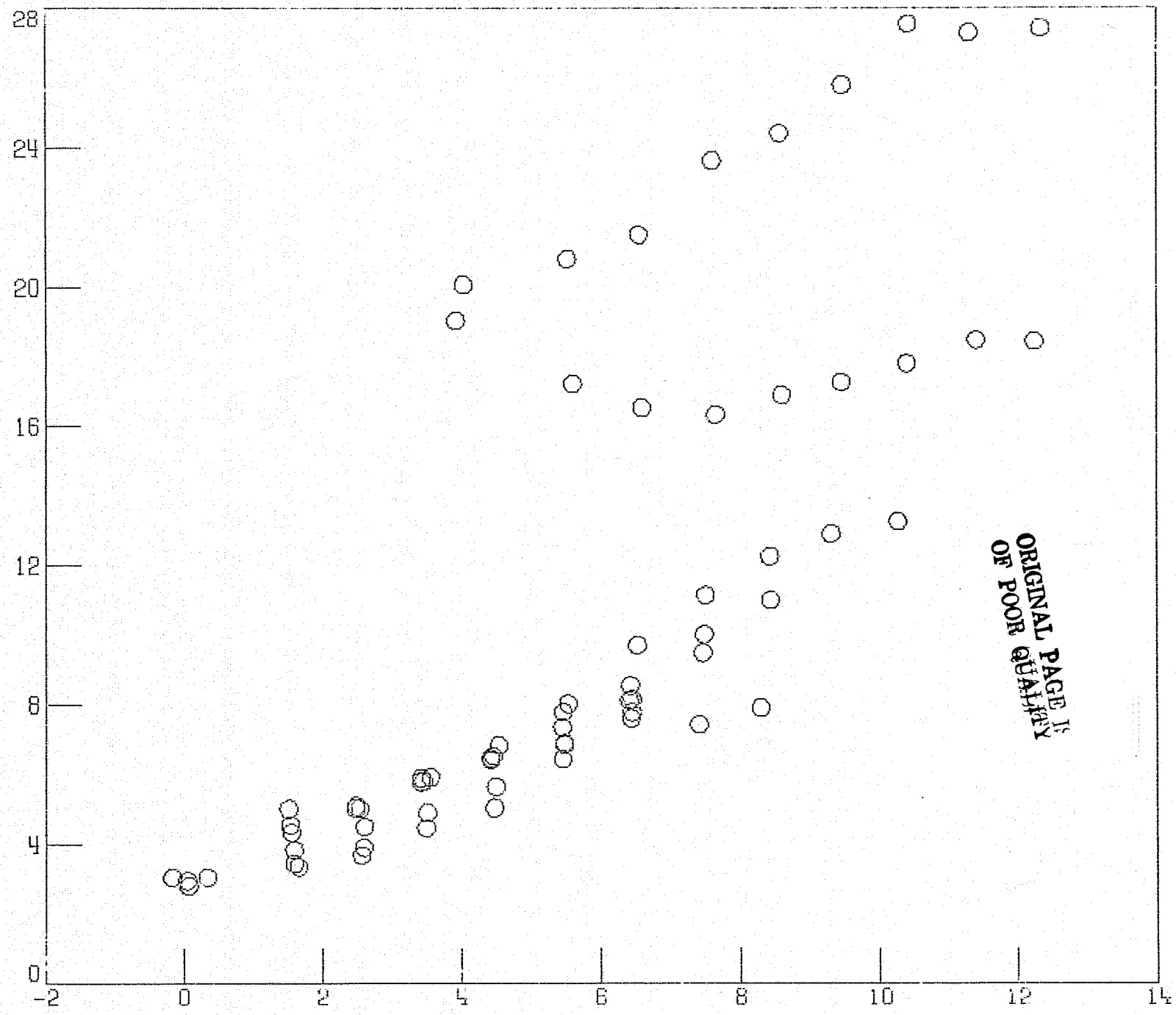

Figure 27. F_1 vs. Iron Concentration, with Both Parameters Calculated from Mean Values of Unadjusted Radiance Data

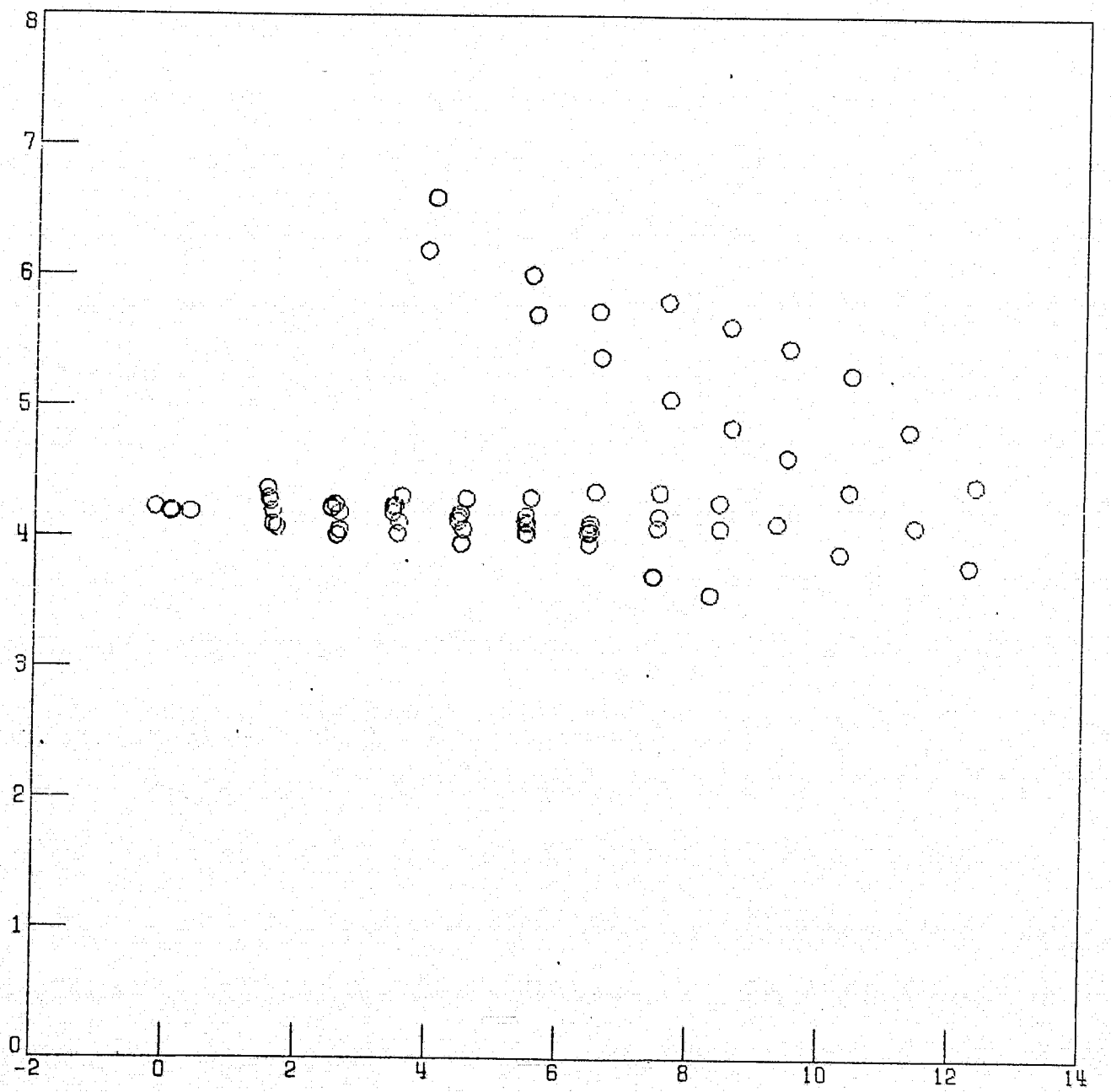

Figure 28. Channel 2 Radiance vs. Iron Concentration from r_2/r_4

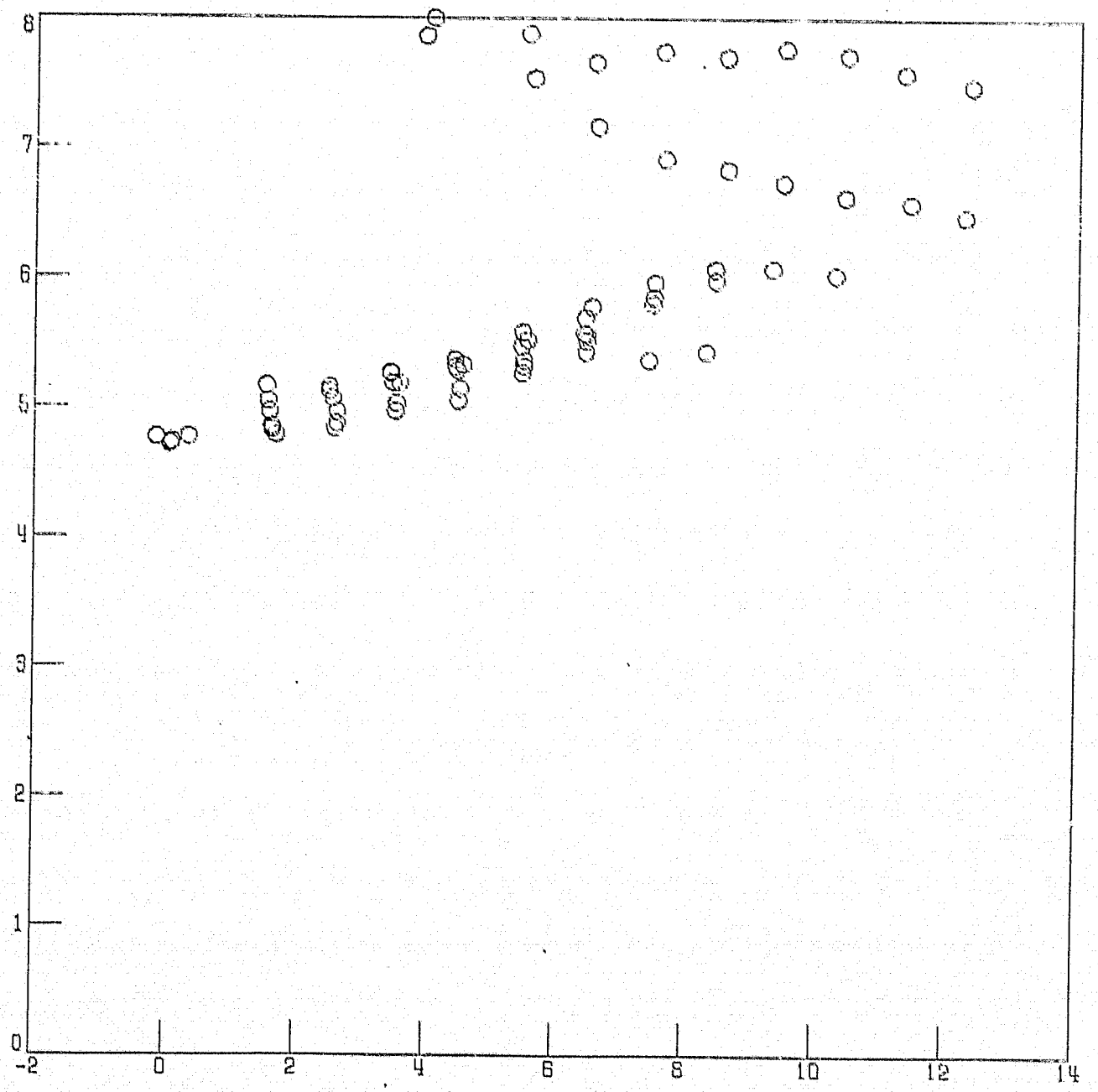

Figure 29. Channel 3 Radiance vs. Iron Concentration from r_2/r_4

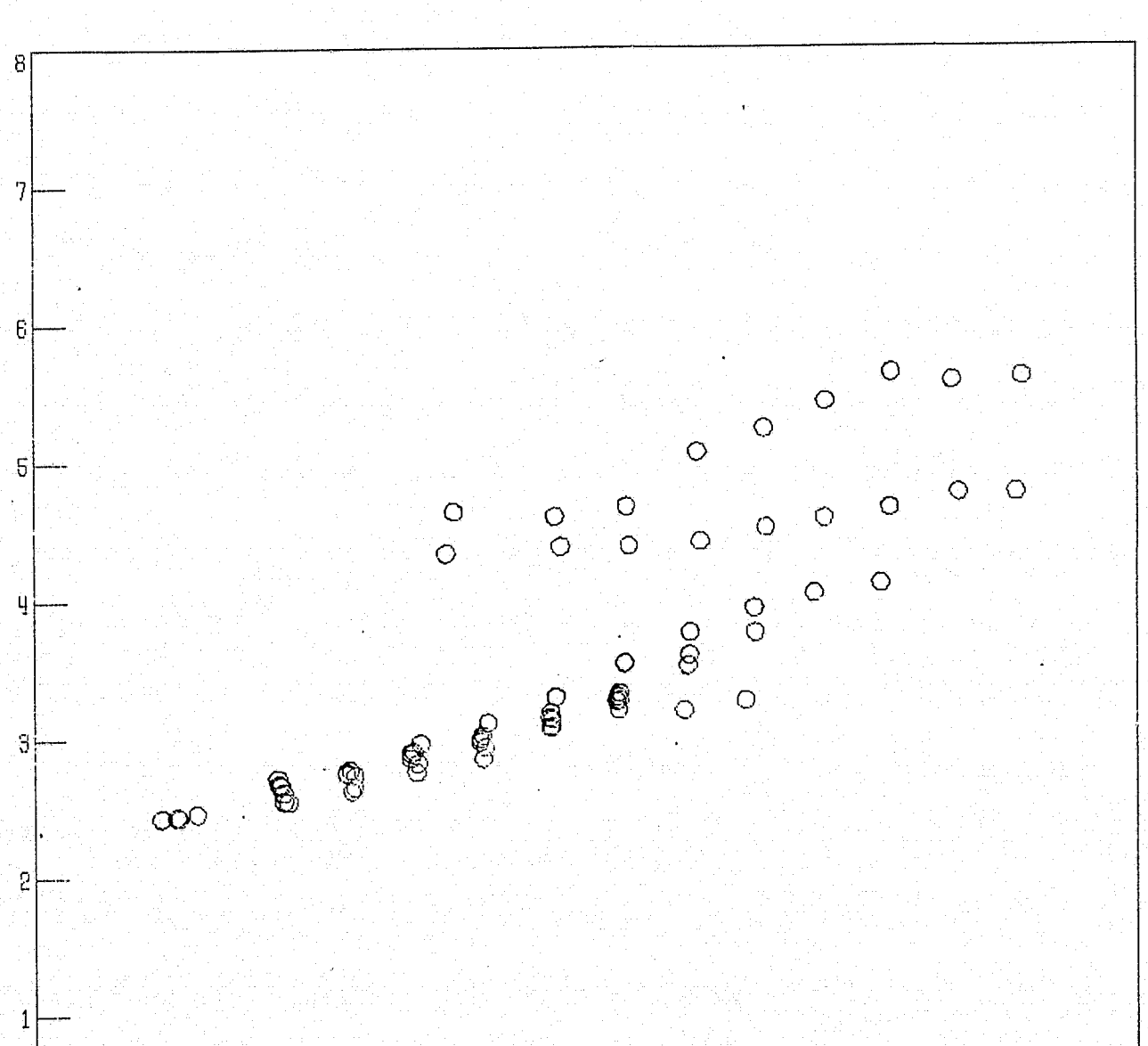

Figure 30. Channel 4 Radiance vs. Iron Concentration from r_2/r_4

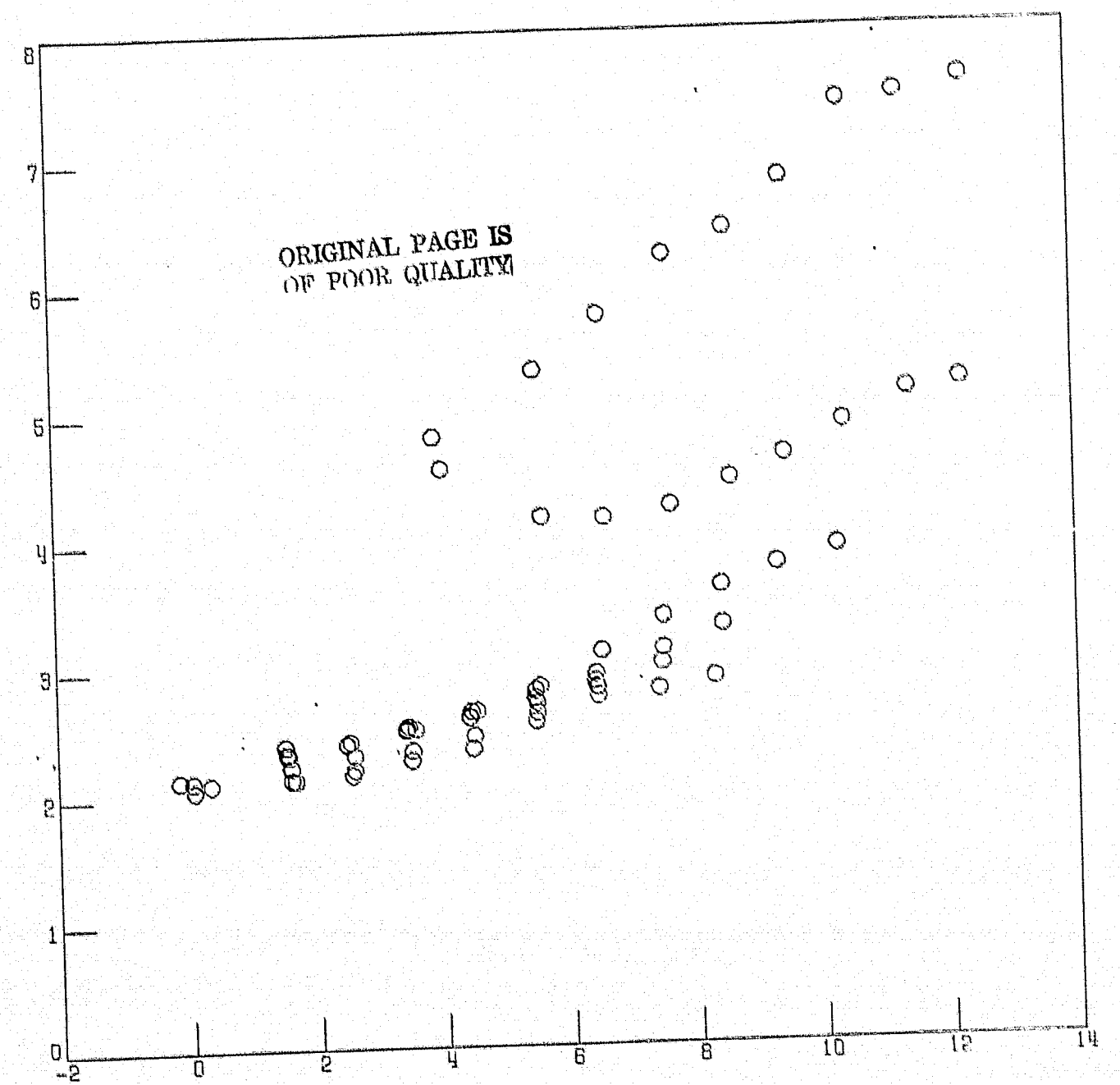

Figure 31. Channel 5 Radiance vs. Iron Concentration from r_2/r_4

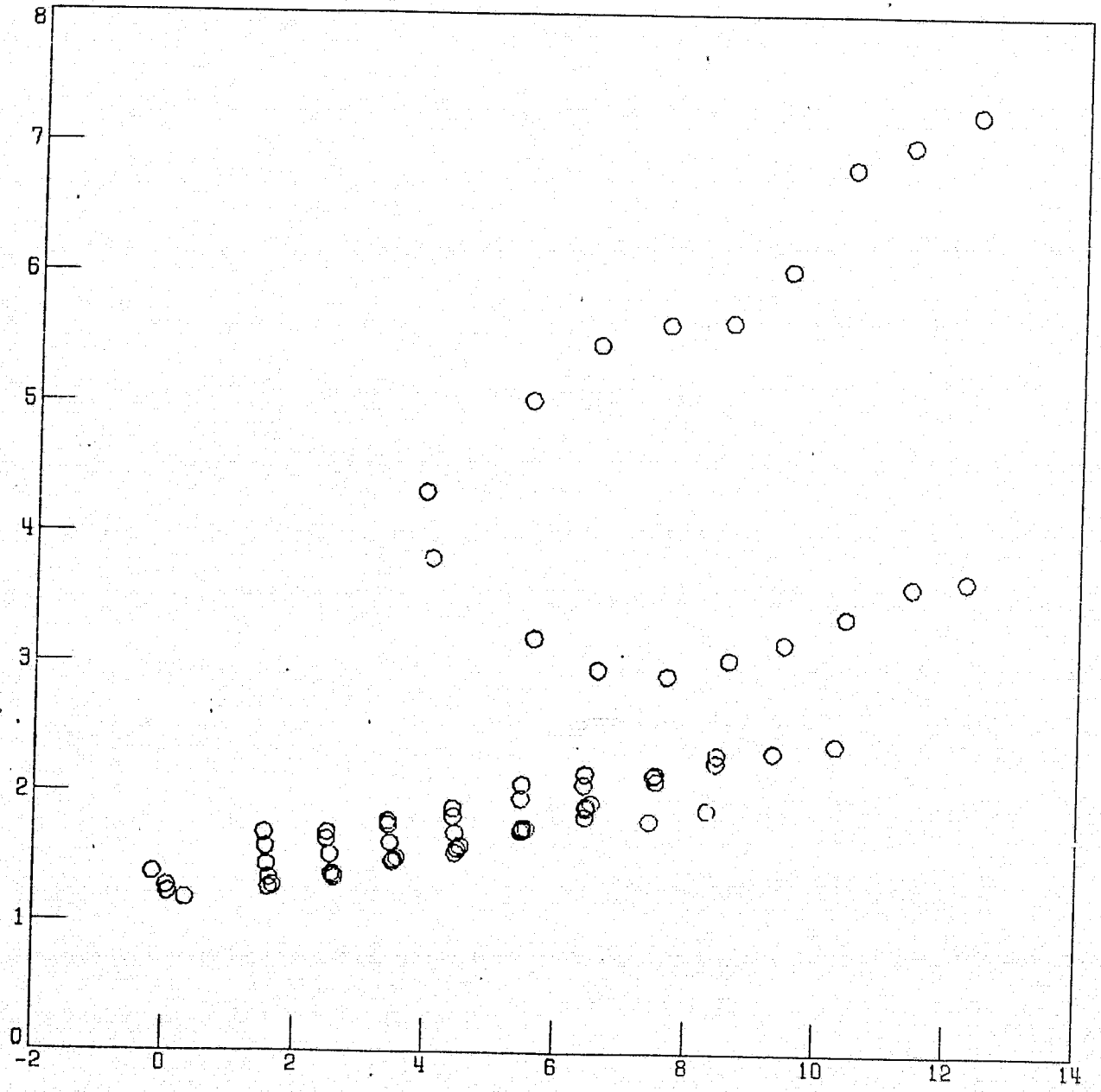

Figure 32. Channel 6 Radiance vs. Iron Concentration from r_2/r_4

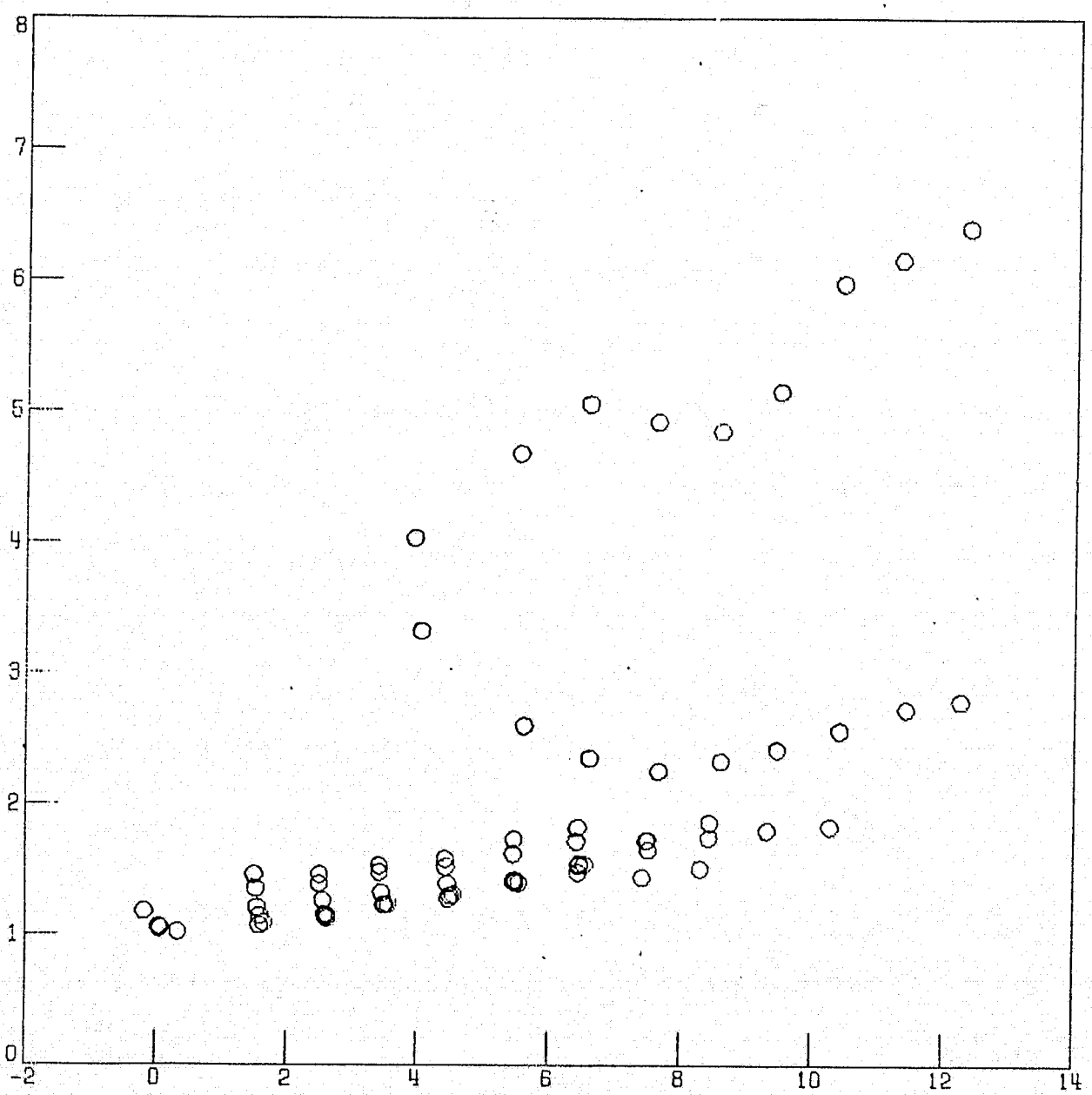

Figure 33. Channel 7 Radiance vs. Iron Concentration from r_2/r_4

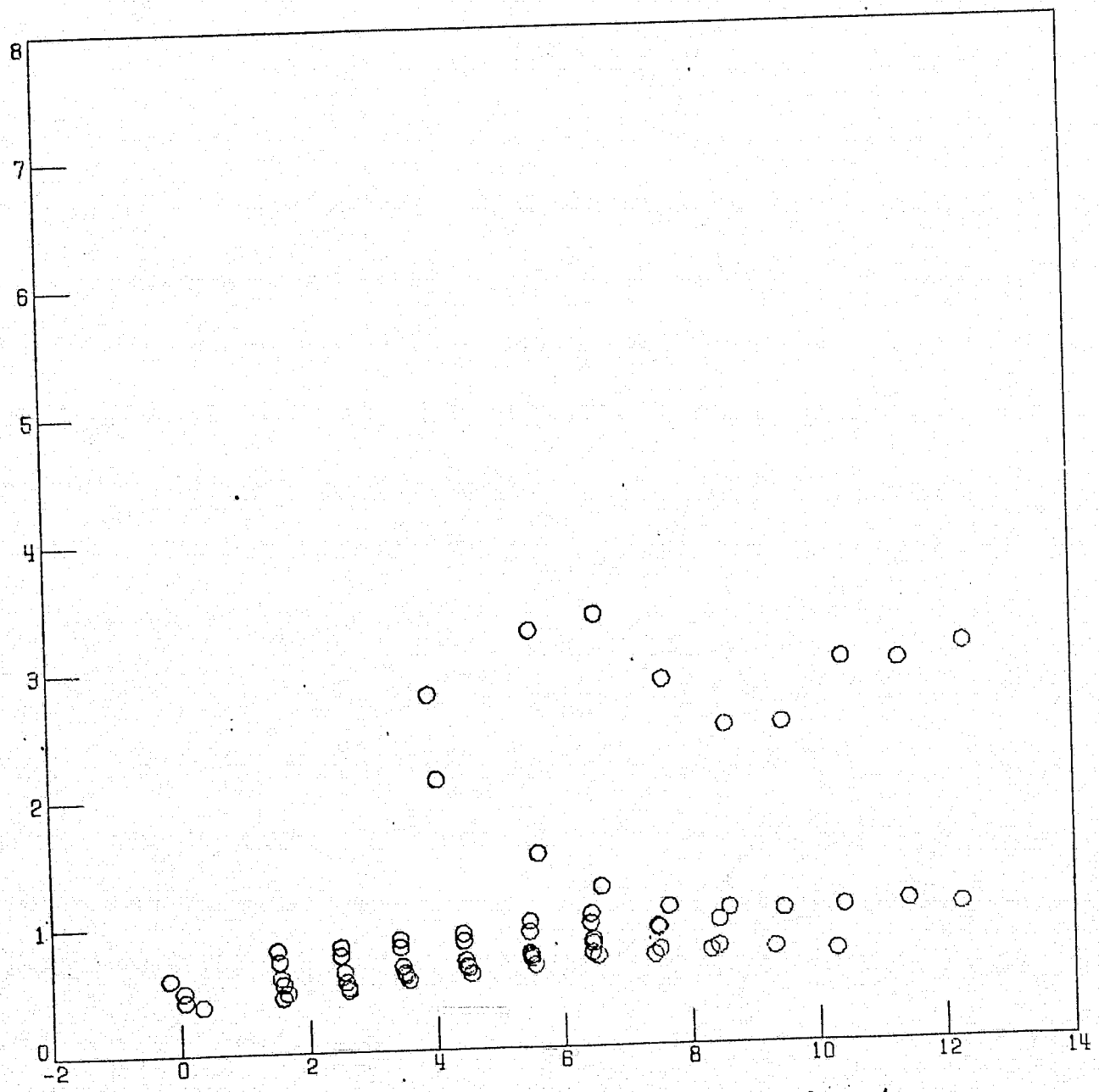

Figure 34. Channel 8 Radiance vs. Iron Concentration from r_2/r_4

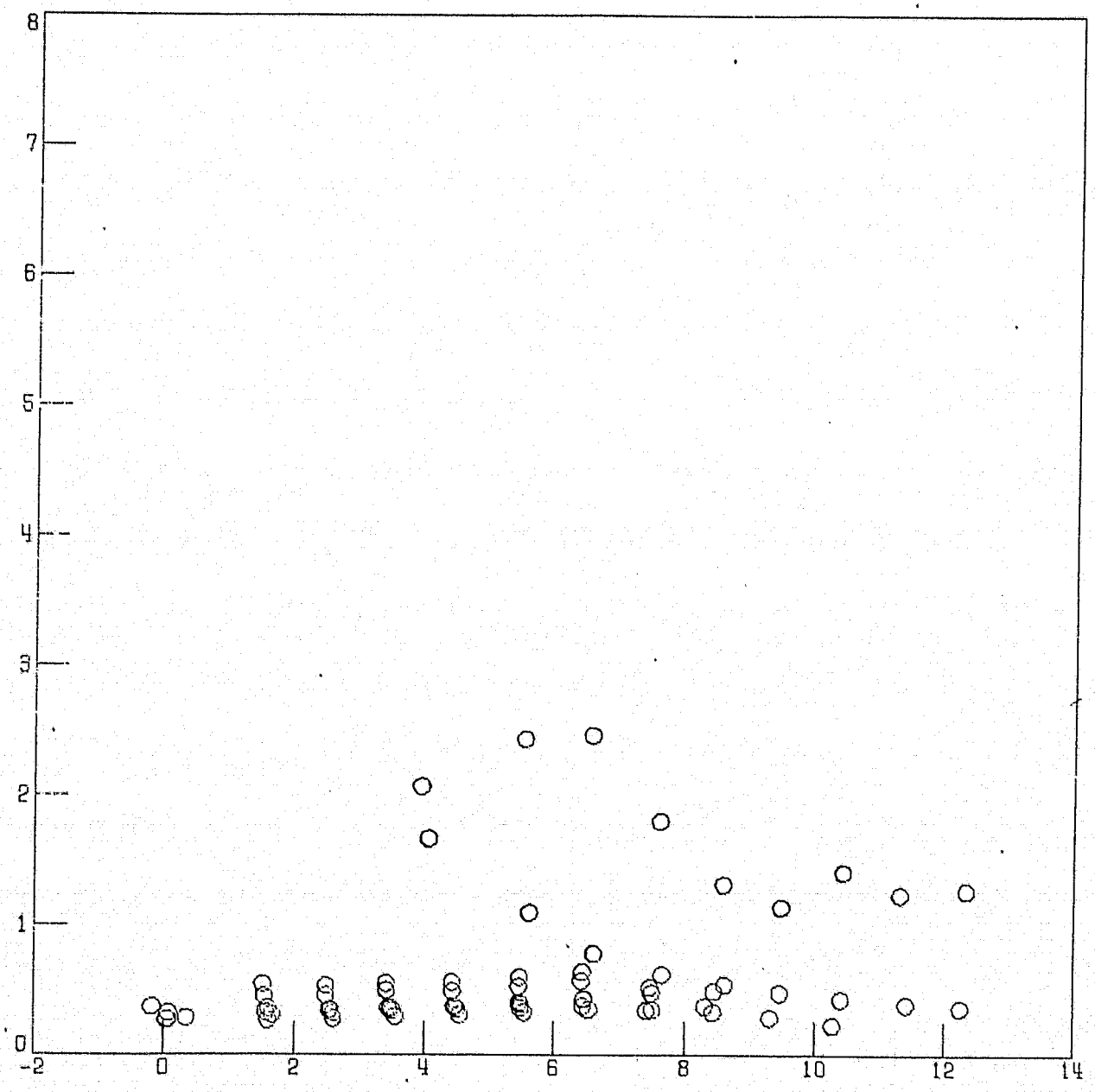

Figure 35. Channel 9 Radiance vs. Iron Concentration from r_2/r_4

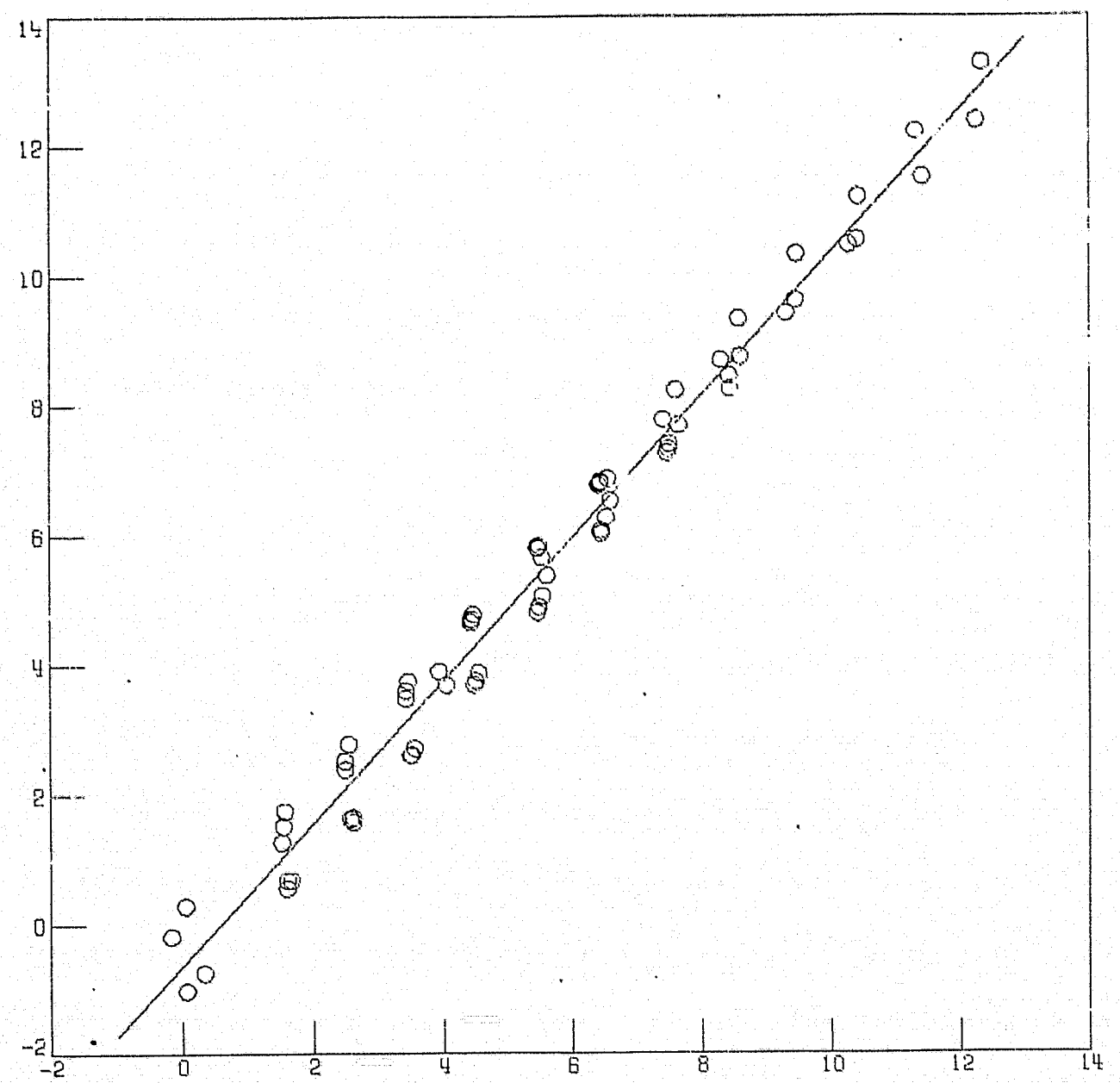

Figure 36. Iron Concentration Calculated from Adjusted Radiances, r_2/r_4, vs. Iron Concentration Calculated from Unadjusted Radiances, r_2/r_4

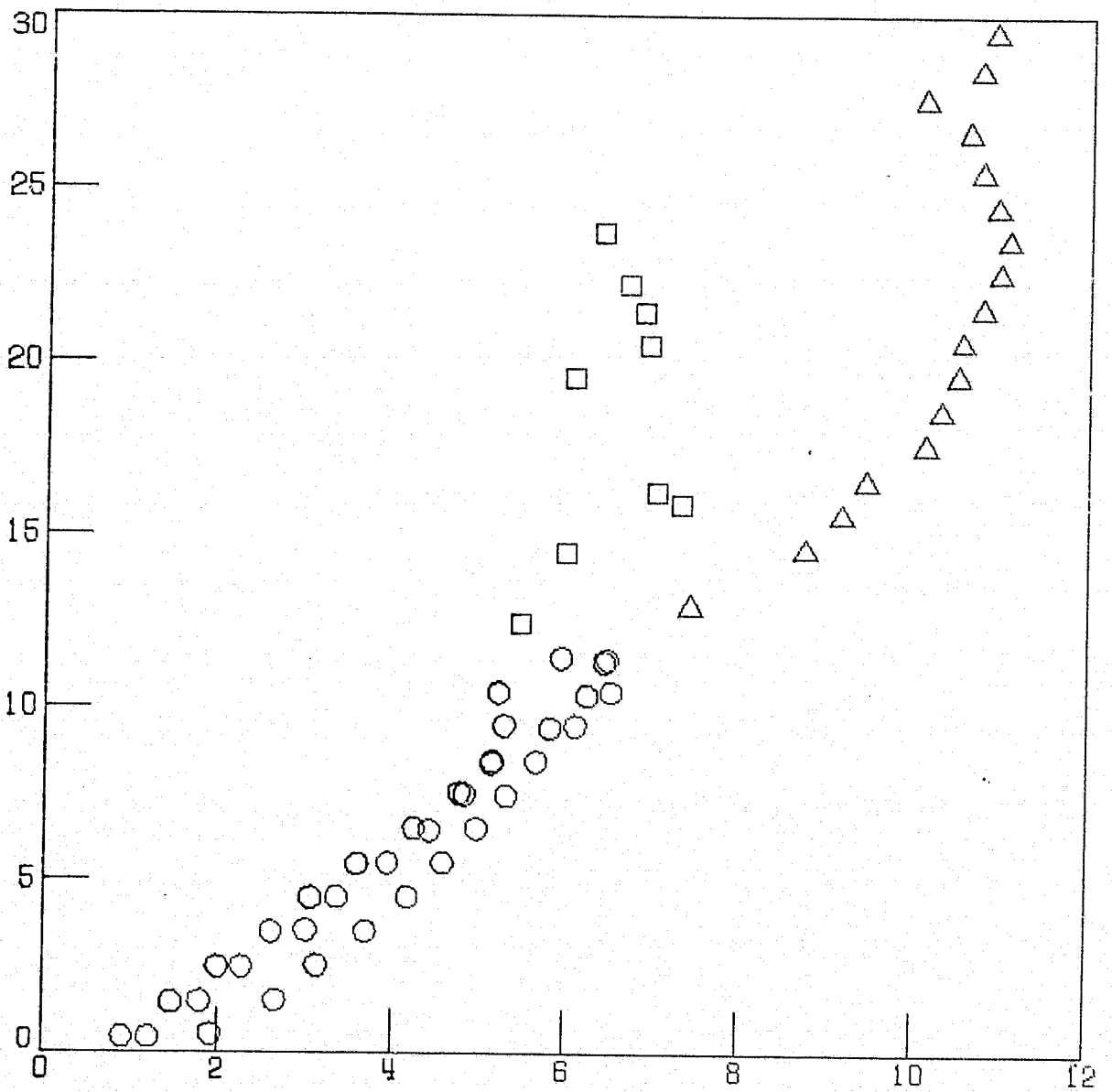

Figure 37. F_1 vs. Fe, Both Calculated from Adjusted Radiances

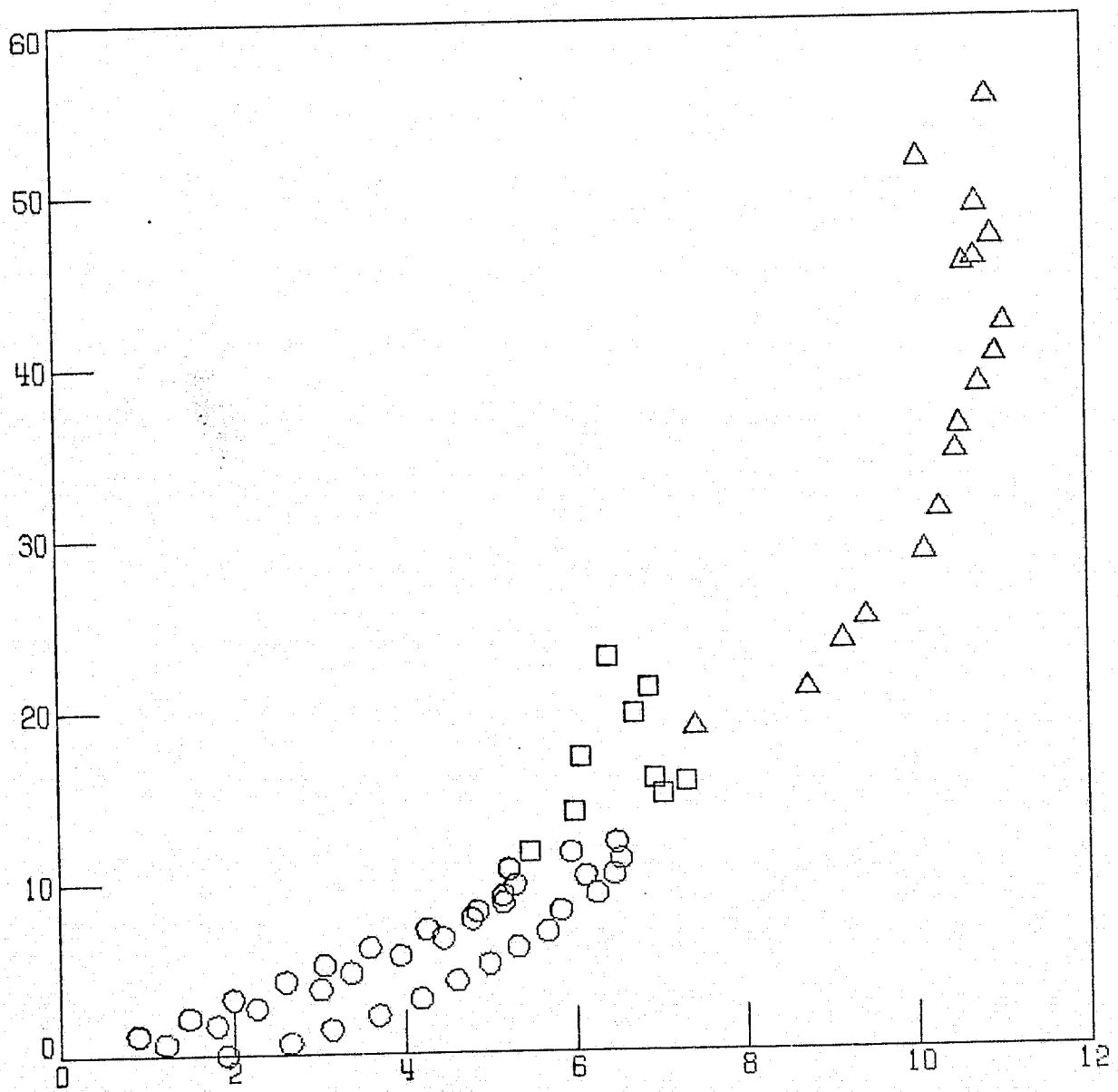

Figure 38. F_2 vs. Fe, Both Calculated from Adjusted Radiances

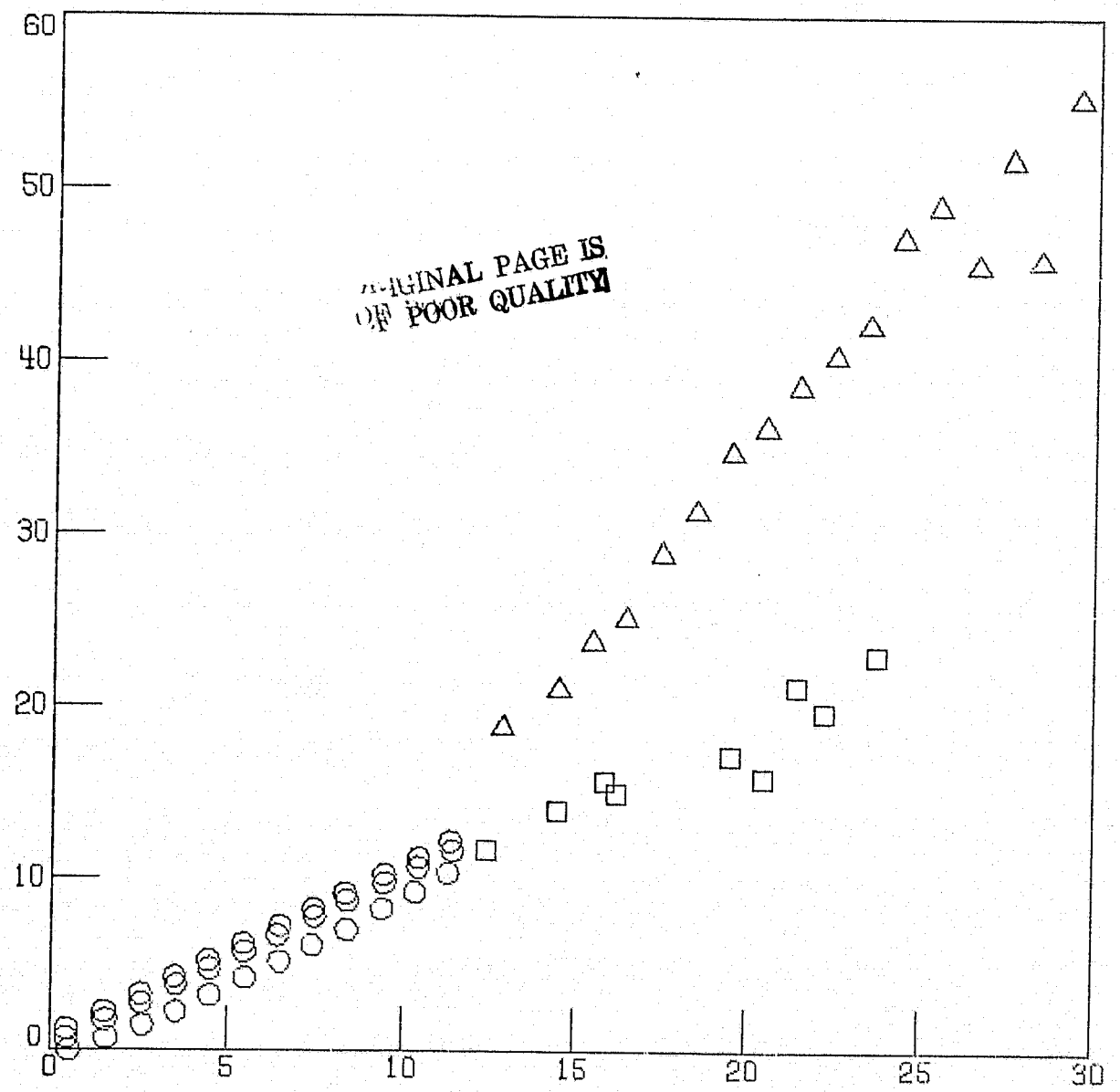

Figure 39. F_2 vs. F_1, Both Calculated from Adjusted Radiances

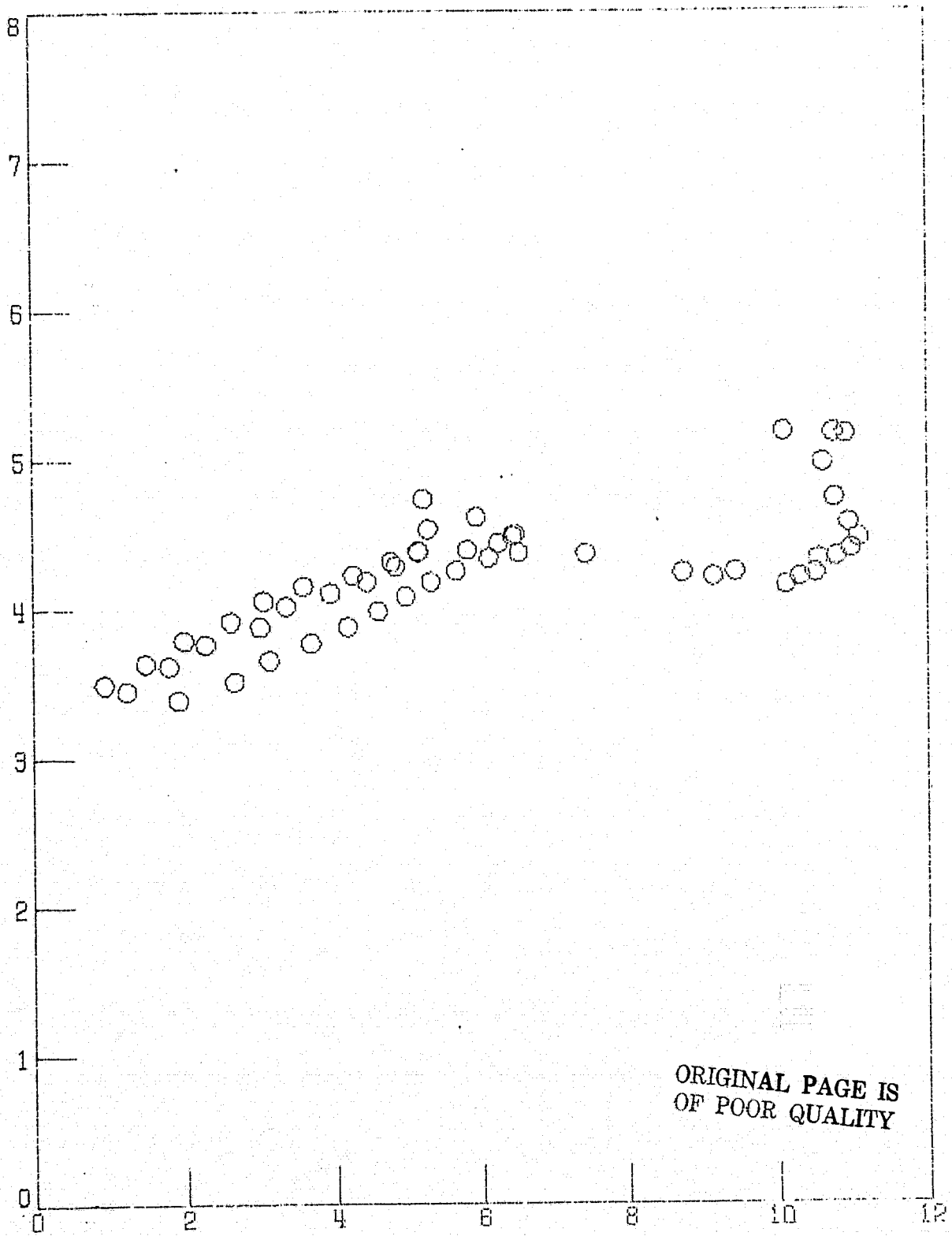

Figure 40. Channel 2 Radiance vs. Fe, with Adjusted Data

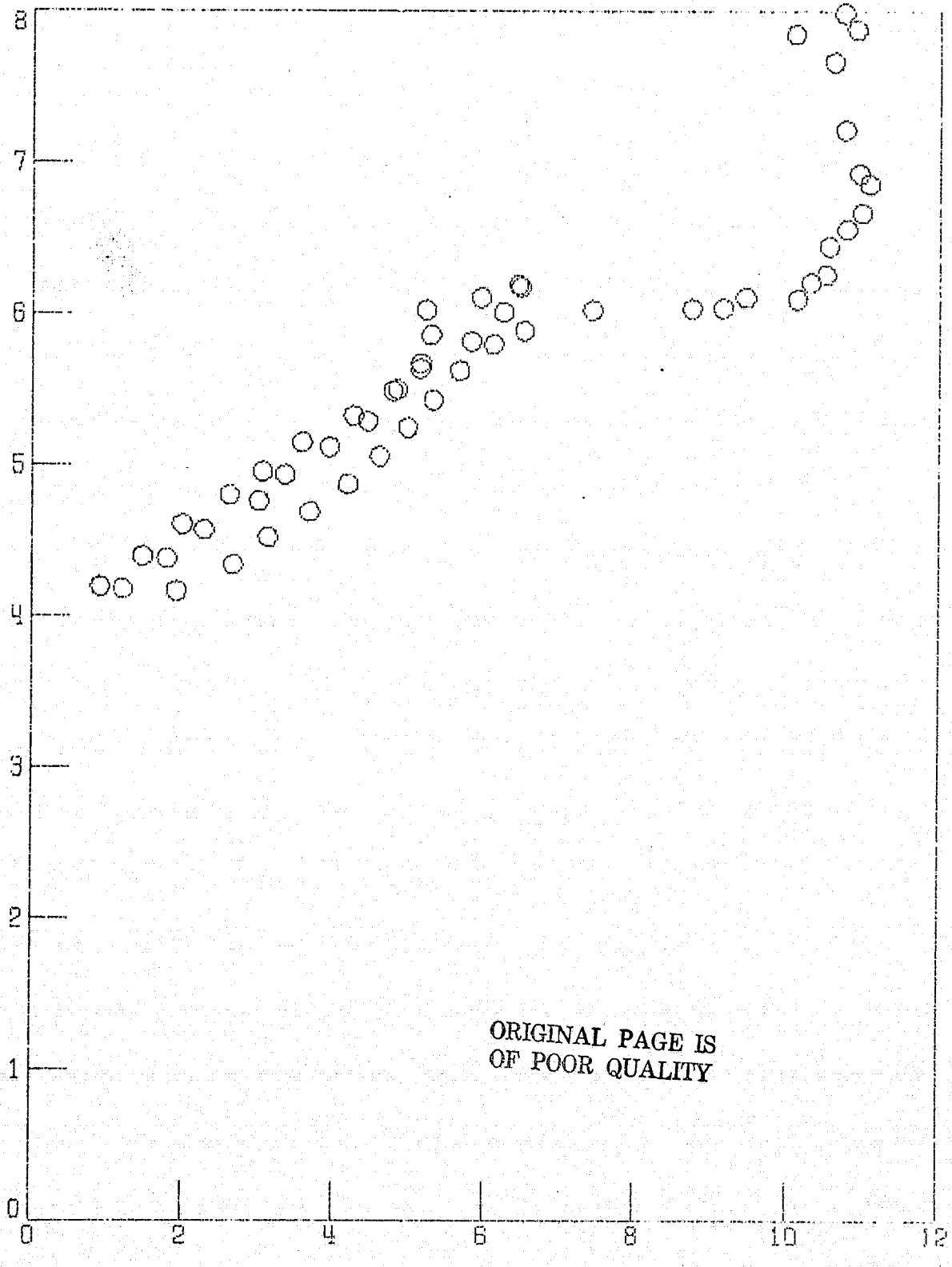

Figure 41. Channel 3 Radiance vs. Fe, with Adjusted Data

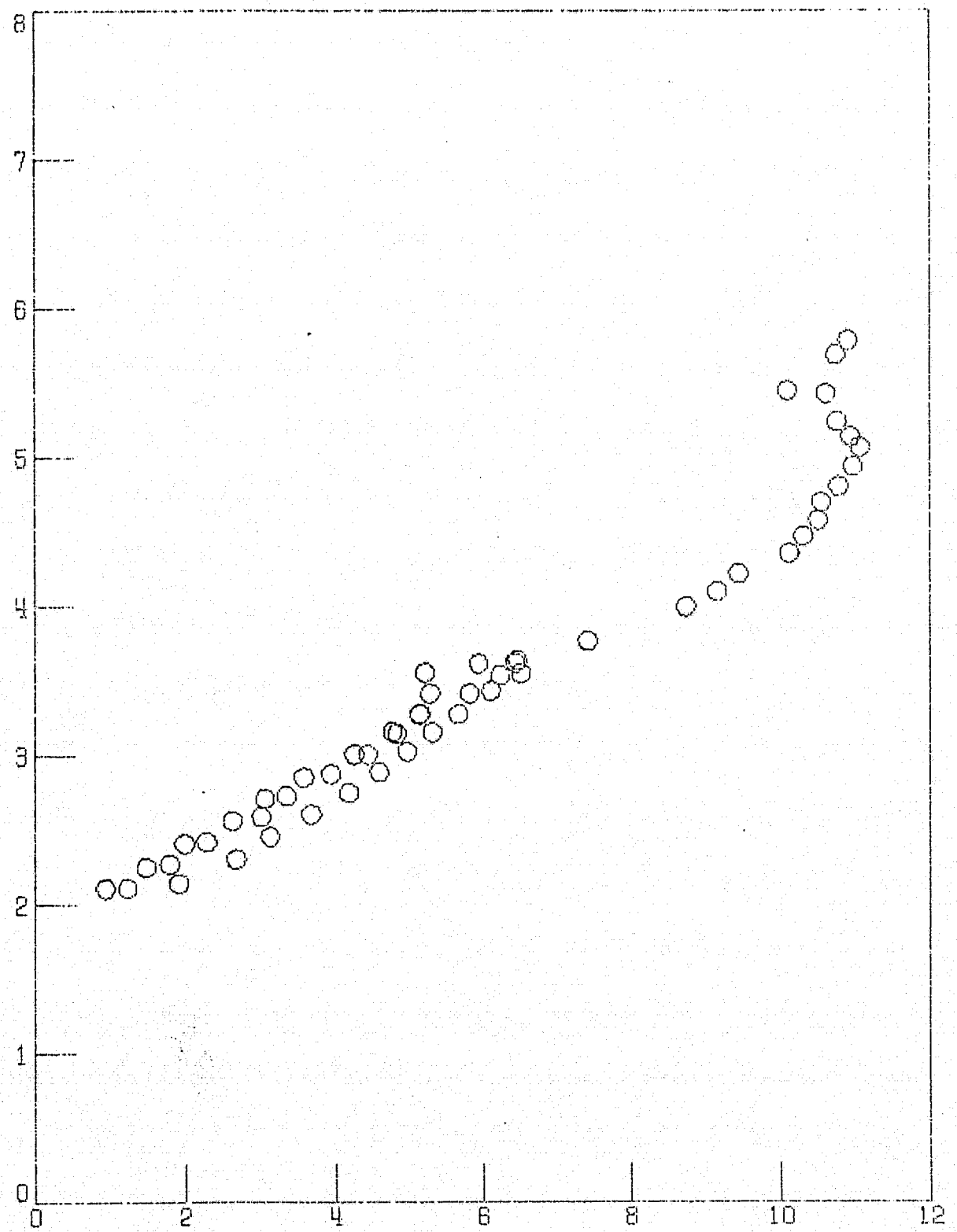

Figure 42. Channel 4 Radiance vs. Fe, with Adjusted Data

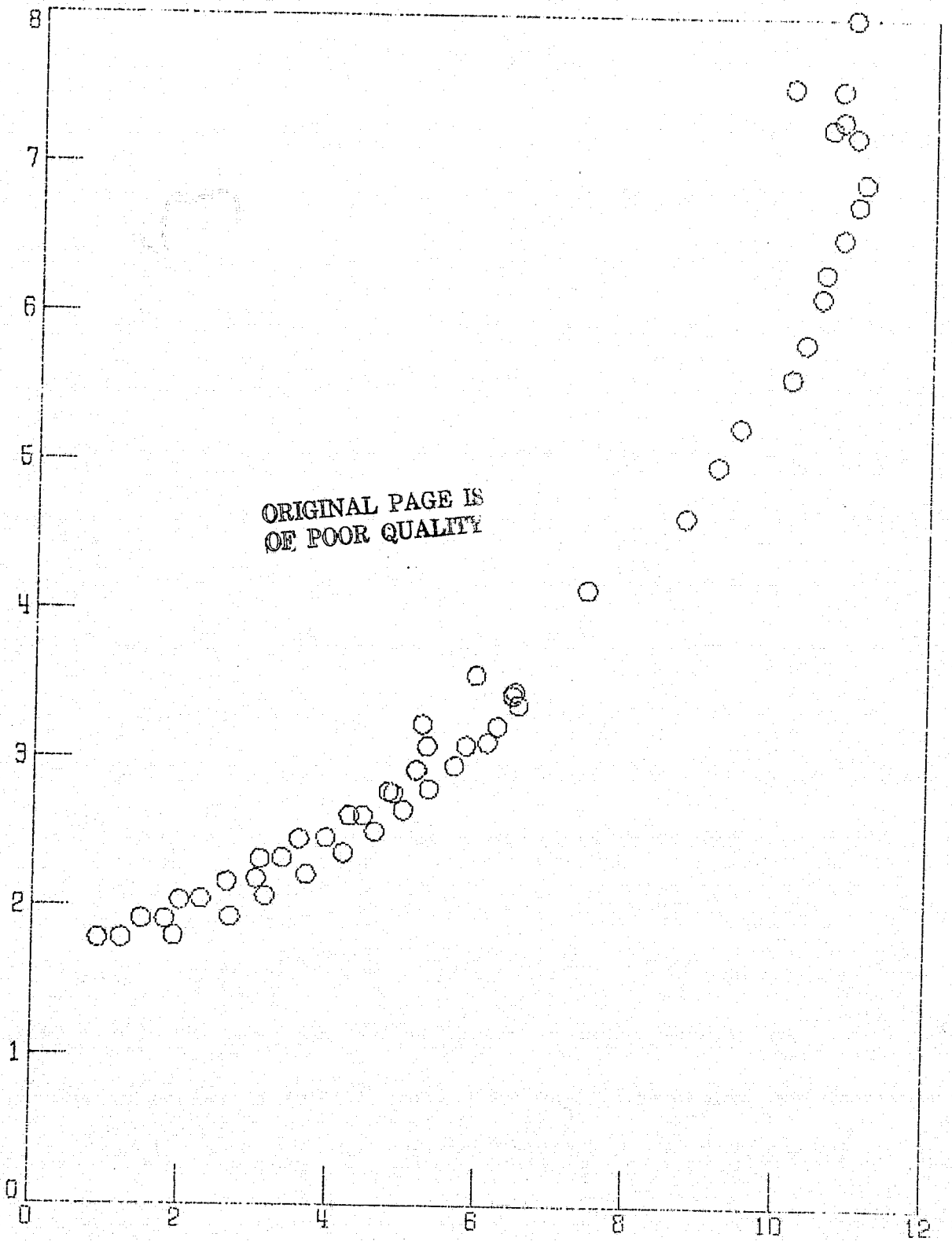

Figure 43. Channel 5 Radiance vs. Fe, with Adjusted Data

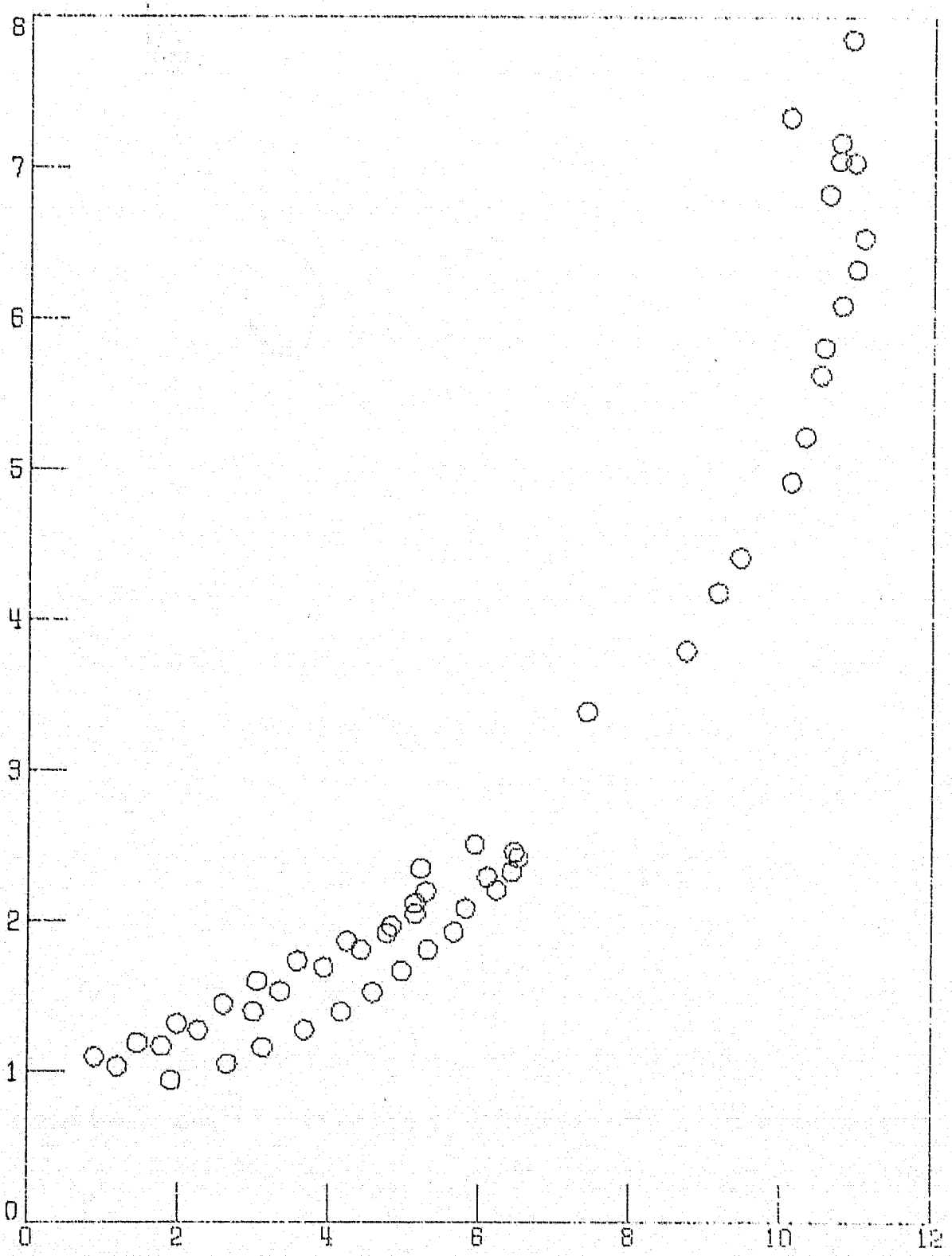

Figure 44. Channel 6 Radiance vs. Fe, with Adjusted Data

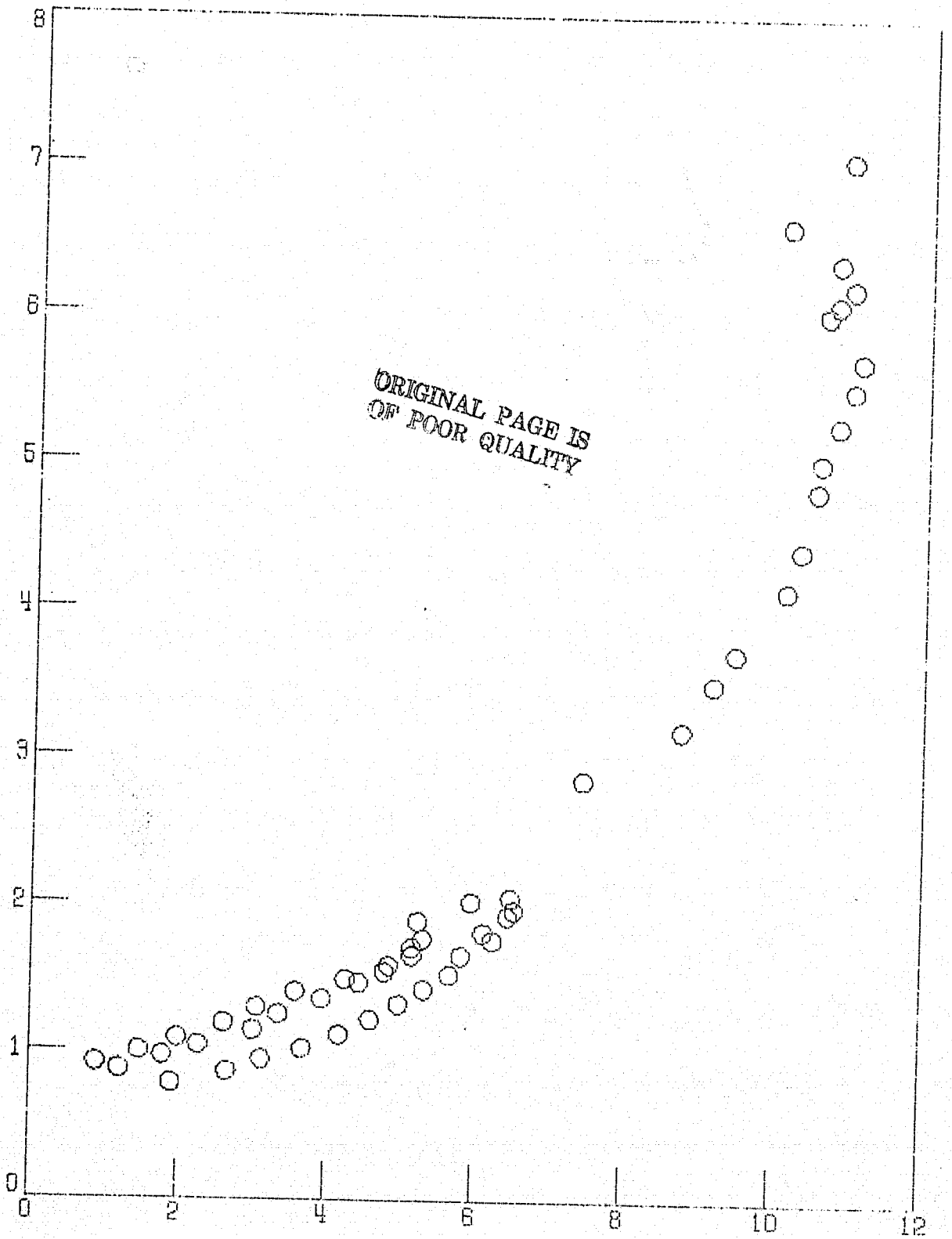

Figure 45. Channel 7 Radiance vs. Fe, with Adjusted Data

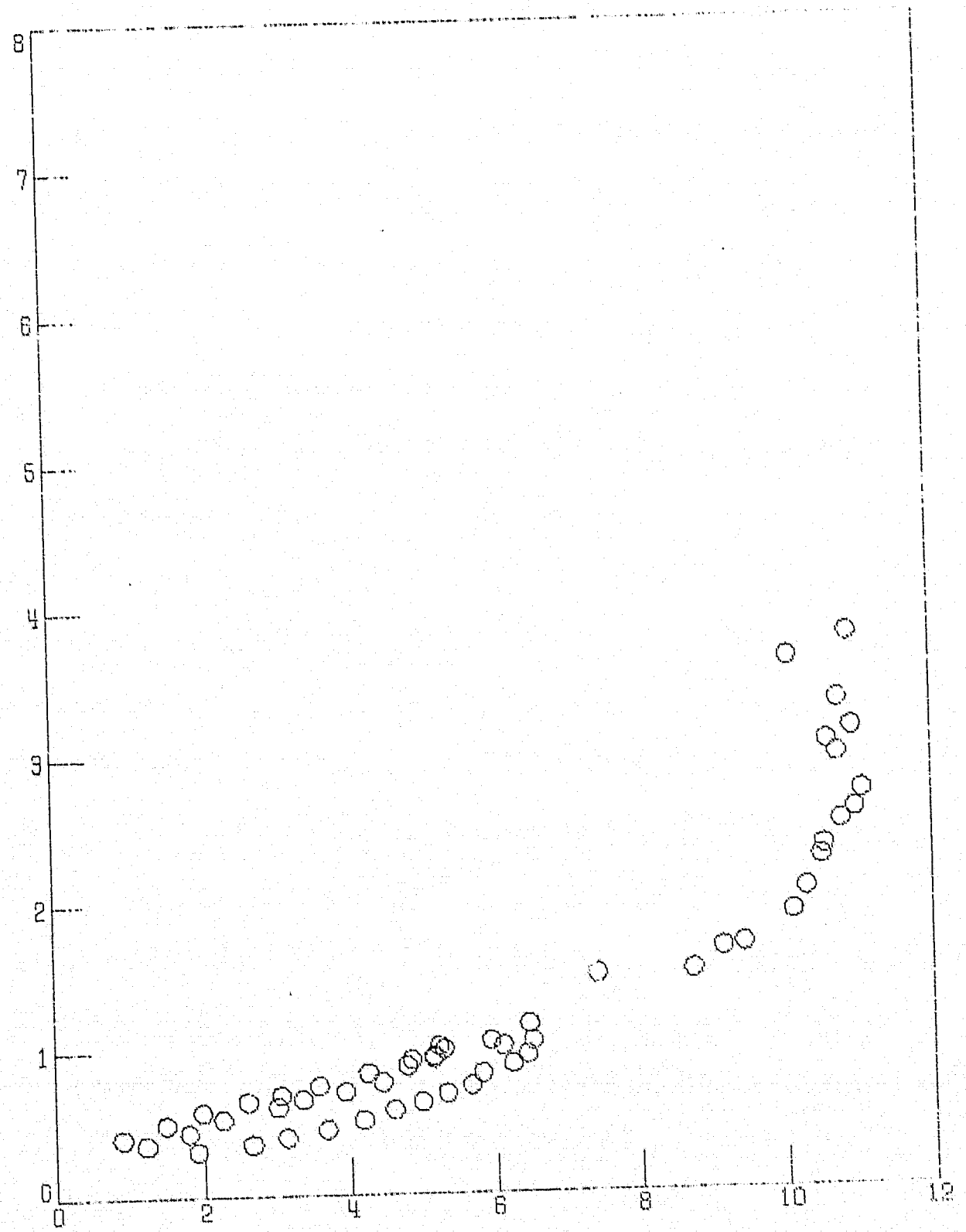

Figure 46. Channel 8 Radiance vs. Fe, with Adjusted Data

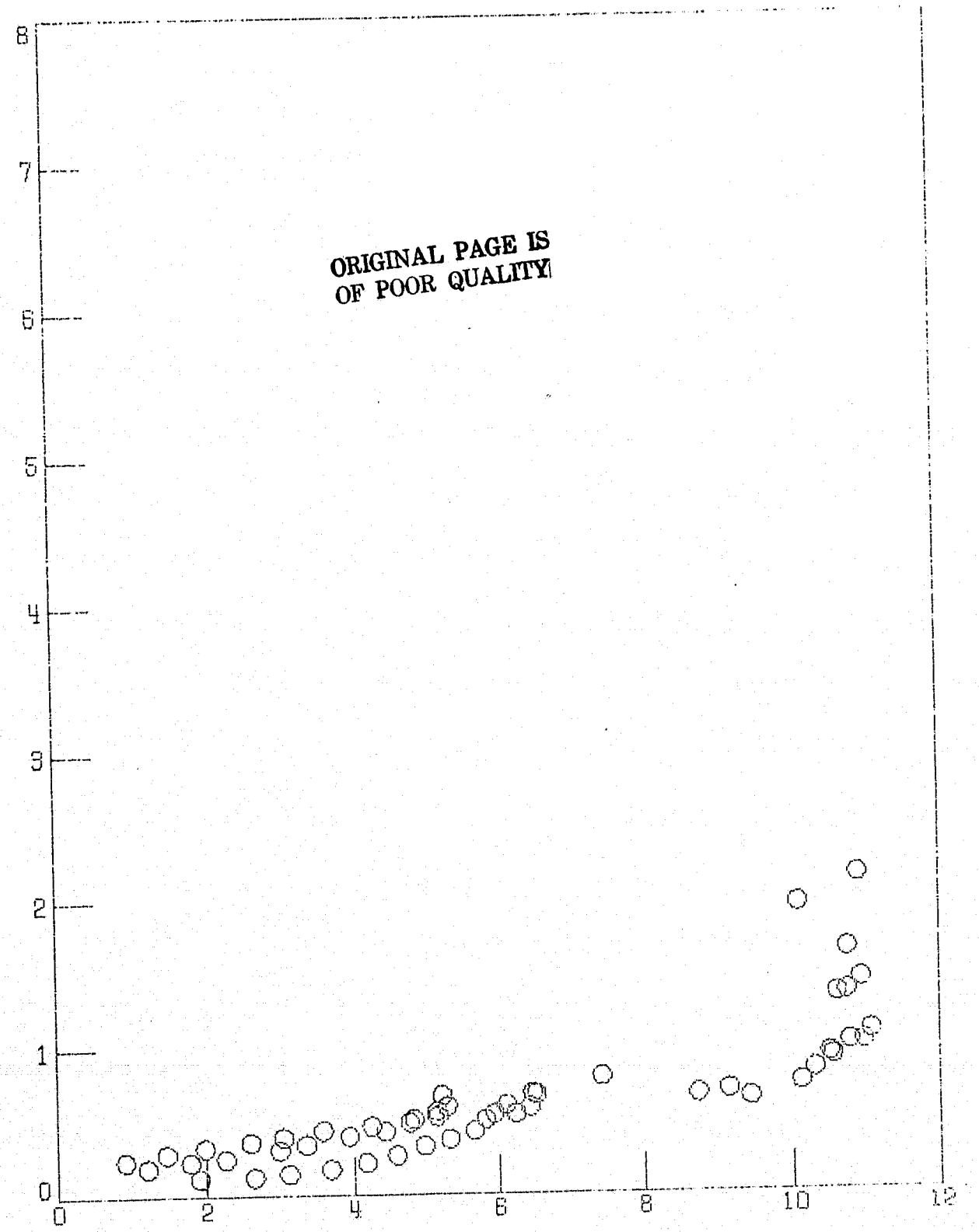

Figure 47. Channel 9 Radiance vs. Fe, with Adjusted Data